Organometallic Molecule-Inorganic Surface Coordination and Catalytic Chemistry. In Situ CPMAS NMR Delineation of Organoactinide Adsorbate Structure, Dynamics, and Reactivity

William C. Finch, Ralph D. Gillespie, David Hedden, and Tobin J. Marks*

Contribution from the Department of Chemistry, Northwestern University, Evanston, Illinois 60208-3113. *Received November 10, 1989*

Abstract: A 75.4-MHz ^{13}C CPMAS NMR spectroscopic study of the surface structures and reaction chemistry of a series of organoactinides adsorbed on various inorganic supports is reported. On Lewis acid surfaces such as dehydroxylated Al_2O_3, $MgCl_2$, and SiO_2-Al_2O_3, it is found that organothorium complexes of the type Cp'_2ThR_2 ($Cp' = \eta^5$-$(CH_3)_5C_5$; R = $^{13}CH_3$, $^{13}CH_2{}^{13}CH_3$), $Cp'ThR_3$ (R = $^{13}CH_2C_6H_5$), and Cp_3ThR ($Cp = \eta^5$-C_5H_5; R = $^{13}CH_3$), undergo heterolytic Th-C scission to transfer an alkyl anion to the surface forming Cp'_2ThR, $Cp'ThR_{3-n}$, or Cp_3Th adsorbate species with "cation-like" character. Probe studies with paramagnetic $Cp'_2U(^{13}CH_3)_2$ indicate that the majority of the transferred methyl groups of $Cp'_2U(^{13}CH_3)_2$/DA and $Cp'_2U(^{13}CH_3)_2/MgCl_2$ are located $\gtrsim$5 Å from the U(IV) ion. On less dehydroxylated or more basic supports such as SiO_2-MgO, SiO_2, and MgO, μ-oxo species of the type $Cp'_2Th(CH_3)O$- are formed, by Th-C protonolysis or by transfer of an alkyl group to the surface. For $Cp'_2U(^{13}CH_3)_2/SiO_2$, the majority of the resulting $^{13}CH_3$-Si(surface) functionalities are $\gtrsim$5 Å from the actinide center. In agreement with heterogeneous catalytic studies, the NMR data reveal that only a small percentage of $Cp'_2Th(^{13}CH_3)_2$/DA or $Cp'Th(^{13}CH_2C_6H_5)_3$/DA surface sites undergo reaction with ethylene or H_2 at 25 °C. In contrast, 50 ± 10% of $Cp'_2Th(^{13}CH_3)_2/MgCl_2$ sites undergo reaction with ethylene; >90 ± 10% of ethylene insertion/polymerization occurs at Th-CH_3 with k(propagation)/k(initiation) ≈ 12 in the initial stages. There is no evidence for methane evolution via C-H functionalization nor for significant rates of $Th(CH_2CH_2)_n{}^{13}CH_3$-$^{13}CH_3Mg$(surface) alkyl group permutation. At 25 °C, a large percentage of $Cp'_2Th(^{13}CH_3)_2/MgCl_2$ Th-CH_3 and Mg-CH_3 functionalities undergo hydrogenolysis, with Th-CH_3 being slightly more reactive. In competition experiments, Th-CH_3 is far more reactive than Mg-CH_3 in migratory CO insertion, and products are inferred to be, inter alia, η^2-acyl complexes. $Cp'_2Th(^{13}CH_3)_2/MgCl_2$ undergoes reaction with propylene to yield methane (derived from Th-CH_3), a Th(η^3-allyl) complex, and what appear to be propylene oligomers.

It is well-established that adsorption on high surface area metal oxides can profoundly enhance the reactivity/catalytic activity of metal hydrocarbyls.[1-3] While such phenomena are of considerable scientific and technological interest, our understanding of the surface coordination chemistry, much less the nature of the active catalytic sites, is at a very primitive level. Moreover, it is not clear that conventional photon/particle absorption, scattering, or diffraction surface science tools[4,5] will be particularly incisive in structurally characterizing such adsorbates on irregular surfaces at less than monolayer coverage.

Recent research in this laboratory has employed organoactinides[6] as model hydrocarbyl adsorbates.[7] Organoactinides have well-defined/controllable oxidation states, useful spectroscopic markers, a diversity of ligational possibilities, and a developing mechanistic/thermochemical foundation. Furthermore, adsorption of molecules such as Cp'_2AnR_2 ($Cp' = \eta^5$-$(CH_3)_5C_5$; An = Th, U; R = alkyl) on dehydroxylated γ-alumina[8] (DA; σ-OH ≈ 0.1 nm^{-2}) affords heterogeneous catalysts with very high activity for olefin hydrogenation and polymerization.[7] In contrast, adsorption upon partially dehydroxylated alumina[8] (PDA; σ-OH ≈ 4 nm^{-2}) or silica[8] (partially dehydroxylated or dehydroxylated; PDS or DS) yields adsorbates with marginal catalytic activity,[7b] while adsorption on $MgCl_2$ affords catalysts with intermediate activity.[7a] Interestingly, quantitative CO or protonolytic poisoning experiments indicate that ~4% of $Cp'_2An(CH_3)_2$/DA and ~35% of $Cp'_2An(CH_3)_2/MgCl_2$ sites are catalytically important in such transformations.[7a,9]

The above catalytic phenomenology suggests an intricate relationship between surface/adsorbate microstructure and activity and one that can only be partially addressed with chemical probes

(1) (a) Iwasawa, Y.; Gates, B. C. *Chemtech* **1989**, *3*, 173-181, and references therein. (b) *Surface Organometallic Chemistry: Molecular Approaches to Surface Catalysis*; Basset, J. M., et al., Eds.; Kluwer: Dordrecht, 1988. (c) Iwasawa, Y. *Adv. Catal.* **1987**, *35*, 187-264. (d) Hartley, F. R. *Supported Metal Complexes: A New Generation of Catalysts*; Reidel: Boston, 1985. (e) McDaniel, M. P. *Adv. Catal.* **1985**, *33*, 47-98. (f) Schwartz, J. *Acc. Chem. Res.* **1985**, *18*, 302-308. (g) Yermakov, Y. I.; Kuznetsov, B. N.; Zakharov, V. A. *Catalysis by Supported Complexes*; Elsevier: Amsterdam, 1981.

(2) (a) Xiaoding, X.; Boelhouwer, C.; Vonk, D.; Benecke, J. I.; Mol, J. C. *J. Mol. Catal.* **1986**, *36*, 47-66, and references therein. (b) Lamb, H. H.; Gates, B. C. *J. Am. Chem. Soc.* **1986**, *108*, 81-89, and references therein. (c) Basset, J. M.; Choplin, A. *J. Mol. Catal.* **1983**, *21*, 95-108, and references therein. (d) Yermakov, Y. I. *J. Mol. Catal.* **1983**, *21*, 35-55, and references therein.

(3) (a) Barbé, P. C.; Cecchin, G.; Noristi, L. *Adv. Polym. Sci.* **1986**, *81*, 1-81. (b) *Catalytic Polymerization of Olefins*; Keii, T., Soga, K., Eds.; Elsevier: Amsterdam, 1986. (c) Myers, D. L.; Lunsford, J. H. *J. Catal.* **1986**, *99*, 140-148, and references therein. (d) Choi, K.-H.; Ray, W. H. *J. Macromol. Sci., Rev. Macromol. Chem. Phys.* **1985**, *C25*, 1-56, 57-97. (e) Pino, P.; Rötzinger, B. *Macromol. Chem. Phys. Suppl.* **1984**, *7*, 41-61. (f) Karol, F. J. *Catal. Rev. Sci. Eng.* **1984**, *26*, 557-595. (g) Firment, L. E. *J. Catal.* **1983**, *82*, 196-212, and references therein.

(4) (a) Van Hove, M. A.; Wang, S.-W.; Ogletree, D. F.; Somarjai, G. A. *Adv. Quantum Chem.* **1989**, *20*, 1-184. (b) Somorjai, G. A. *Chemistry in Two Dimensions: Surfaces*; Cornell University Press: Ithaca, 1981; Chapters 2 and 5. (c) *Spectroscopy in Hetereogeneous Catalysis*; Delgass, W. N., Haller, G. L., Kellerman, R., Lunsford, J. H., Eds.; Academic Press: New York, 1979.

(5) Metal hydride functionalities can sometimes be detected by vibrational spectroscopy in such systems.[1g,3g]

(6) (a) Marks, T. J.; Streitwieser, A., Jr. In *The Chemistry of the Actinide Elements*, 2nd ed.; Katz, J. J., Seaborg, G. T., Morss, L. R., Eds.; Chapman and Hall: London, 1986; Chapter 22. (b) Marks, T. J. *Ibid.* Chapter 23.

(7) (a) Gillespie, R. D.; Burwell, R. L., Jr.; Marks, T. J. *Langmuir* In press. (b) He, M.-Y.; Xiong, G.; Toscano, P. J.; Burwell, R. L., Jr.; Marks, T. J. *J. Am. Chem. Soc.* **1985**, *107*, 641-652. (c) Burwell, R. L., Jr.; Marks, T. J. In *Catalysis of Organic Reactions*; Augustine, R. L., Ed.; Marcel Dekker, Inc.: New York, 1985; pp 207-224. (d) He, M.-Y.; Burwell, R. L., Jr.; Marks, T. J. *Organometallics* **1983**, *2*, 566-569. (e) Xiong, G.; Burwell, R. L., Jr.; Marks, T. J. Unpublished results.

(8) (a) Kijenski, J.; Balker, A. *Catalysis Today* **1989**, *5(1)*, 1-120. (b) Knözinger, H. in ref 1b, Chapter 1. (c) Beránek, L.; Kraus, M. In *Comprehensive Chemical Kinetics*; Bamford, C. H., Tipper, C. F. H., Eds.; Elsevier: Amsterdam, 1978; pp 263-398. (d) Benesi, H. A.; Winquist, B. H. C. *Adv. Catal.* **1978**, *27*, 97-182. (e) Knözinger, H.; Ratnasamy, P. *Catal. Rev.-Sci. Eng.* **1978**, *17*, 31-70. (f) Lippens, B. C.; Steggerda, J. J. In *Physical and Chemical Aspects of Adsorbents and Catalysts*; Linsen, B. G., Ed.; Academic Press: London, 1970; Chapter 4. (g) Schwarz, J. A. *J. Vac. Sci. Technol.* **1975**, *12(1)*, 321-323. (h) Tanabe, K. *Solid Acids and Bases*; Kodansha: Tokyo, Academic Press: New York, 1970.

(9) That less than 100% of surface sites are catalytically significant is a common phenomenon in heterogeneous catalysis. See, for example: (a) Rooney, J. J. *J. Mol. Catal.* **1985**, *31*, 137-159, and references therein. (b) Boudart, M. *J. Mol. Catal.* **1985**, *30*, 27-37, and references therein.

0002-7863/90/1512-6221$02.50/0

(e.g., tracing the origin of methane evolved during adsorption).[7b] In this context, high-resolution solid-state NMR spectroscopy[10] offers considerable promise as a surface structural tool,[11] and in our earliest 15 MHz ^{13}C CPMAS studies of $Cp'_2Th(^{13}CH_3)_2$/DA, we detected an unprecedented transfer of a methyl group to an Al site on the surface (A).[12a] The Lewis acid character of the

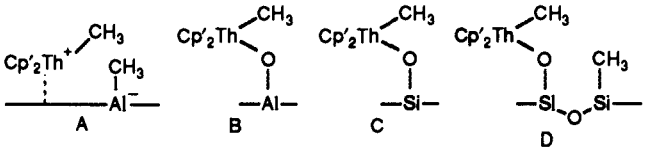

surface receptor sites, spectral similarities to cationic $Cp'_2Th(CH_3)^+BPh_4^-$/$Cp'_2Th(CH_3)(THF)_2^+BPh_4^-$ complexes,[13] and growing evidence that Cp'_2ThR^+-like species will be highly reactive[11e,14] suggested that A has electrophilic, "cation-like" character. In contrast, the negligible catalytic activity of $Cp'_2Th(CH_3)_2$ on PDA, PDS, and DS, along with spectral similarities to unreactive $Cp'_2Th(CH_3)OR$ compounds,[15] suggests different, "μ-oxo-like" adsorbate structures B, C, and D, respectively.[12] Nevertheless, these preliminary oxide support results leave many questions unanswered. From a descriptive, coordination chemistry standpoint, the generality of this picture in regard to support (other oxides, halides) and complex (other precursor structures) is unclear. Whether A might be a μ-alkyl,[16] E, whether Th–R and Al–R groups can interchange,[16] and what the reactivity of such surface functionalities is with respect to olefins, H_2, CO, etc., remain to be answered. Finally, the relevance of the above phenomenology to the observed catalytic properties and the structural models to the actual catalytic sites are unexplored.

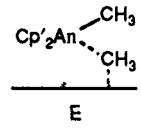

E

In the present contribution, we present a full discussion of our high field (75.4 MHz), high-resolution solid-state ^{13}C NMR investigations of supported organoactinide structural and surface chemistry.[17,18] This includes a full examination of a range of supports (Al_2O_3, $MgCl_2$, SiO_2–Al_2O_3, SiO_2–MgO, MgO) and metal complexes (Cp'_2AnR_2, $Cp'AnR_3$, Cp_3AnR), in situ chemical dosing/adsorbate reactivity studies, and the use of paramagnetic U(IV) adsorbates in a new approach to probing metrical aspects of the surface complexation. It is seen that this integrated chemical/spectroscopic approach affords a far more complete picture of this unusual but, in all likelihood, generalizable[1-3] surface organometallic chemistry. Moreover, important connections are demonstrated between the heterogeneous catalytic phenomenology and the spectroscopic structure/reactivity observations.

Experimental Section

Materials and Methods. All procedures were performed in Schlenk-type glassware interfaced to a high-vacuum (10^{-4}–10^{-5} Torr) line or in a nitrogen-filled Vacuum Atmospheres glovebox equipped with an efficient recirculating atmosphere purification system (typically 2–3 ppm O_2). Argon (Matheson, prepurified), hydrogen (Linde), and CO (Matheson CP) were purified further by passage through MnO/Vermiculite and Davison 4A molecular sieves. Other gases including propylene (Matheson), ethylene (Matheson), ethylene-*1,2*-$^{13}C_2$ (99% ^{13}C; Cambridge Isotopes), CO-^{13}C (99% ^{13}C; Cambridge Isotopes), and propylene-2-^{13}C (60% ^{13}C; MSD Isotopes) were purified by passage through MnO/SiO_2. The 3,3-dimethylbutene (Aldrich) was dried over Na/K, vacuum transferred into a storage tube equipped with a Teflon valve, and stored under an argon atmosphere. Pentane (Aldrich HPLC grade) was vacuum transferred from either Na/K or CaH_2 and stored in vacuo over Na/K in bulbs on the vacuum line.

The compounds $^{13}CH_3Li$-LiI,[12a] $Cp'_2Th(CH_3)_2$,[19] $Cp'_2Th(^{13}CH_3)_2$,[12a] $Cp_3Th(CH_3)$,[20] $[Cp'_2Th(\mu\text{-}H)H]_2$,[19] $Cp'Th(CH_2C_6H_5)_3$,[21] $Cp'_2Th(CH_2CH_3)_2$,[19] and $Cp'_2Th(CH_2CH_2CH_2CH_3)_2$[22] were prepared according to published procedures. $Cp'_2Th(^{13}CH_2{}^{13}CH_3)_2$ was prepared from $[Cp'_2Th(\mu\text{-}H)H]_2$ and 90% ethylene-*1,2*-$^{13}C_2$,[19] and $Cp_3Th(^{13}CH_3)$ was synthesized from Cp_3ThCl and $^{13}CH_3Li$-LiI.[20] By using the synthetic procedure for $Cp'Th(CH_2C_6H_5)_3$,[21] $Cp'Th(^{13}CH_2C_6H_5)_3$ was prepared from $C_6H_5{}^{13}CH_2Li$ and $Cp'ThCl_3(THF)_2$. The reagent, $C_6H_5{}^{13}CH_2Li$, was in turn prepared from $C_6H_5{}^{13}CH_3$ and *n*-butyllithium;[23] the ^{13}C labeled toluene was prepared from $C_6H_5{}^{13}COOH$ (Cambridge Isotope, 99% ^{13}C).[24] The complex $Cp'_2U(^{13}CH_3)_2$ was prepared from Cp'_2UCl_2 and $^{13}CH_3Li$-LiI by using the method for $Cp'_2U(CH_3)_2$.[19] The purity of these reagents was checked by ^1H NMR.

The supports DA and DS were prepared as previously described.[7,12] Magnesium chloride (surface area $\approx$ 100 $m^2\ g^{-1}$) was supplied by Dow Chemical Co. and was pretreated under high vacuum (10^{-5} Torr), 300°, 2 (this code indicates heating at 300 °C for 2 h). Alternatively, $MgCl_2$ was prepared by reaction of dibutylmagnesium (Lithium Corp. of America) with HCl (Matheson VLSI grade) in pentane by using greaseless high vacuum line techniques (surface area $\approx$ 100 $m^2\ g^{-1}$). It was again pretreated under high vacuum, 300°, 2. SiO_2–Al_2O_3 (Davison 970 grade, 13% Al_2O_3, 60–80 mesh material) was purified by the same procedure as for PHF Al_2O_3,[12] followed by treatment in flowing He, 950°, 0.5 (surface area $\approx$ 56 $m^2\ g^{-1}$). Partially dehydroxylated MgO (Calgon Maglite CG-1) was treated in flowing He, 680°, 0.5 (surface area $\approx$ 46 $m^2\ g^{-1}$). and SiO_2–MgO (Grace SM-30) was treated in flowing He, 800°, 0.5 (surface area $\approx$ 275 $m^2\ g^{-1}$). All supports were stored in vacuum-tight glass storage tubes under an inert nitrogen atmosphere.

Impregnation of Supports with Organoactinide Complexes. In a two-sided, fritted reaction vessel interfaced to the high vacuum line, a pentane

(10) (a) Gerstein, B. C.; Dybowski, C. R. *Transient Techniques in NMR of Solids*: Academic Press: Orlando, FL, 1985. (b) Fyfe, C. A. *Solid State NMR for Chemists*; CRC Press: Guelph, 1983. (c) Yannoni, C. S. *Acc. Chem. Res.* **1982**, *15*, 201–208. (d) Duncan, T. M.; Dybowski, C. *Surf. Sci. Rep.* **1981**, *1*, 157–250.

(11) For recent applications of ^{13}C CPMAS NMR to the characterization of organotransition-metal adsorbates and heterogeneous catalysts, see: (a) Weiss, K.; Lössel, G. *Angew. Chem., Int. Ed. Engl.* **1989**, *28*, 62–64. (b) Anderson, M. W.; Klinowski, J. *Nature* **1989**, *339*, 200–203. (c) Haw, J. F.; Richardson, B. R.; Oshiro, I. S.; Lazo, N. D.; Speed, J. A. *J. Am. Chem. Soc.* **1989**, *111*, 2052–2058. (d) Walter, T. H.; Thompson, A.; Keniry, M.; Shinoda, S.; Brown, T. L.; Gutowsky, H. S.; Oldfield, E. *J. Am. Chem. Soc.* **1988**, *110*, 1065–1068. (e) Dahmen, K. H.; Hedden, D.; Burwell, R. L., Jr.; Marks, T. J. *Langmuir* **1988**, *4*, 1212–1214. (f) Toscano, P. J.; Marks, T. J. *Organometallics* **1986**, *5*, 400–402.

(12) (a) Toscano, P. J.; Marks, T. J. *J. Am. Chem. Soc.* **1985**, *107*, 653–659. (b) Toscano, P. J.; Marks, T. J. *Langmuir* **1986**, *2*, 820–823.

(13) Synthesis, characterization, and chemistry of Cp'_2ThR^+ complexes: (a) Lin, Z.; LeMarechal, J. F.; Sabat, M.; Marks, T. J. *J. Am. Chem. Soc.* **1987**, *109*, 4127–4129. (b) Lin, Z.; LeMarechal, J. F.; Yang, X.-M.; Sabat, M.; Marks, T. J. Manuscript in preparation. (c) Marks, T. J. *Abstracts of Papers*; 197th National Meeting of the American Chemical Society, Dallas, TX; American Chemical Society: Washington, DC, April 9–14, 1989; INOR 8.

(14) (a) Hlatky, G. G.; Turner, H. W.; Eckman, R. R. *J. Am. Chem. Soc.* **1989**, *111*, 2728–2729. (b) Jordan, R. F.; LaPointe, R. E.; Bradley, P. K.; Baenziger, N. *Organometallics* **1989**, *8*, 2892–2903. (c) Gassman, P. G.; Callstrom, M. R. *J. Am. Chem. Soc.* **1987**, *109*, 7875–7876. (d) Jordon, R. F.; Echols, S. F. *Inorg. Chem.* **1987**, *26*, 383–386. (e) Jordan, R. F.; LaPointe, R. F.; Bagjur, C. S.; Echols, S. F.; Willett, R. *J. Am. Chem. Soc.* **1987**, *103*, 4111–4113. (f) Jordan, R. F.; Bagjur, C. S.; Dasher, W. E.; Rheingold, A. L. *Organometallics* **1987**, *6*, 1041–1051. (g) Jordan, R. F.; Bajgur, C. S.; Willett, R.; Scott, B. *J. Am. Chem. Soc.* **1986**, *108*, 7410–7411. (h) Jordan, R. F.; Dasher, W. E.; Echols, S. F. *J. Am. Chem. Soc.* **1986**, *108*, 1718–1719.

(15) (a) Lin, Z.; Marks, T. J. *J. Am. Chem. Soc.* In press. (b) Lin, Z.; Marks, T. J. *J. Am. Chem. Soc.* **1987**, *109*, 7979–7985.

(16) (a) Holton, J.; Lappert, M. F.; Pearce, R.; Yarrow, P. I. W. *Chem. Rev.* **1983**, *83*, 135–201, and references therein. (b) Evans, W. J.; Chamberlain, L. R.; Ulibarri, T. A.; Ziller, J. W. *J. Am. Chem. Soc.* **1988**, *110*, 6423–6432. (c) Busch, M. A.; Harlow, R.; Watson, P. L. *Inorg. Chem. Acta* **1987**, *140*, 15–20. (d) Holton, J.; Lappert, M. F.; Ballard, D. G. H.; Pearce, R.; Atwood, J. L.; Hunter, W. E. *J. Chem. Soc., Dalton Trans.* **1979**, 54–61. (e) Holton, J.; Lappert, M. F.; Ballard, D. G. H.; Pearce, R.; Atwood, J. L.; Hunter, W. E. *J. Chem. Soc., Dalton Trans.* **1979**, 45–53. (f) Huffman, J. C.; Streib, W. E. *J. Chem. Soc., Chem. Commun.* **1971**, *911*.

(17) For preliminary communication of some aspects of $Cp'_2Th(CH_3)_2$/$MgCl_2$ surface chemistry, see: Hedden, D.; Marks, T. J. *J. Am. Chem. Soc.* **1988**, *110*, 1647–1649.

(18) For a preliminary communication of related organozirconium surface chemistry, see ref 11e.

(19) Fagan, P. J.; Manriquez, J. M.; Maatta, E. A.; Seyam, A. M.; Marks, T. J. *J. Am. Chem. Soc.* **1981**, *103*, 6650–6667.

(20) Bruno, J. W.; Kallna, D. G.; Mintz, E. A.; Marks, T. J. *J. Am. Chem. Soc.* **1982**, *104*, 1860–1869.

(21) Mintz, E. A.; Moloy, K. G.; Marks, T. J.; Day, V. W. *J. Am. Chem. Soc.* **1982**, *104*, 4692–4695.

(22) (a) Bruno, J. W.; Marks, T. J.; Morss, L. R. *J. Am. Chem. Soc.* **1983**, *105*, 6824–6832. (b) Sonnenberger, D. A.; Morss, L. R.; Marks, T. J. *Organometallics* **1985**, *4*, 352–355.

(23) (a) Moloy, K. G. Ph.D. Thesis, Northwestern University, 1985. (b) *Chem. Abstr.* **1971**, *74*, 3723b.

(24) Benkeser, R. A. *J. Am. Chem. Soc.* **1970**, *92*, 3232–3233.

solution containing a measured quantity of the organoactinide complex of interest was filtered onto a carefully weighed quantity of support. The resulting slurry was then stirred for at least 2 h with exclusion of light. The slurry was next filtered, and the impregnated support was collected on the glass frit. This material was then washed with 5 × 5 mL portions of pentane distilled and condensed from the filtrate and was dried in vacuo. Maximum loadings of organoactinides on $MgCl_2$ were ~0.25 An/nm^2, while higher loadings (~0.5 An/nm^2) are achievable on DA and DS.

Reactions of Supported Organoactinides with Small Molecules. The following experiment is illustrative of the procedure used. In the recirculating glovebox, Cp′$_2$Th($^{13}CH_3$)$_2$/DA (1.5 g, 160 μmol Th) was spread on the bottom of a 250-mL Erlenmeyer flask. The flask was equipped with a Teflon valve adapter through which it could be interfaced to the high vacuum line. The flask was sealed, removed from the glovebox, connected to the vacuum line, and evacuated. The vessel was then cooled to 77 K, and a measured quantity of ethylene was admitted. The flask was maintained at 77 K for 30 min and was then allowed to warm slowly to room temperature while continuously monitoring the pressure. At ca. −10 °C, uptake of ethylene began. After ensuring that the reaction was complete (4 h at room temperature), the flask was evacuated to remove any volatiles, resealed, and returned to the glovebox so that an NMR sample could be prepared. Reactions of CO, ^{13}CO, propylene, 60% propylene-2-^{13}C, and 3,3-dimethylbutene were conducted in the same way. For reactions with hydrogen, the procedure was modified such that after the initial evacuation of the flask containing the supported organoactinide, it was filled to ca. 1 atm with hydrogen and sealed off. After the desired reaction time, the excess hydrogen was removed in vacuo.

High-Resolution Solid-State ^{13}C NMR Spectroscopy. All ^{13}C solid-state NMR spectra were recorded on a Varian VXR300 spectrometer (75.4 MHz) equipped with either a Doty Scientific 7 mm or 5 mm high speed solids probe. High-power ^1H decoupling (~65 kHz decoupling field), cross-polarization (CP), and magic angle spinning (MAS) were employed for routine experiments. Air-sensitive samples were loaded into cylindrical sapphire rotors in the glovebox. The rotors were capped at both ends with either O-ring sealed Macor caps (7- and 5-mm rotors) or Kel-F caps (5-mm rotors only). Both types of caps provide an air-tight seal under nonspinning conditions. MAS was achieved by using boil-off nitrogen as the spinning gas to prevent sample exposure to air. Spinning rates of 3.5–4.2 kHz were routinely achieved with the 7-mm probe. With the 5-mm probe, spinning rates of up to 8.5 (Macor rotor caps) and 10.0 kHz (Kel-F caps) could be achieved. Control experiments using highly sensitive samples that undergo distinct color changes upon oxidation (NaC_5H_5; Cp′$_2$U(CH_3)$_2$/DA) or in which the rotor cap was briefly removed in air (to determine oxidation-induced spectral changes) indicated negligible sample deterioration in this spinning configuration over time periods as long as 72 h. For both probes, the magic angle was initially set by using neat KBr. The stability of the angle setting was routinely monitored by observing the aromatic carbon line shape of neat hexamethylbenzene. Spectra were referenced to tetramethylsilane (δ 0) by using the aromatic carbon resonance of hexamethylbenzene (δ 132.1) as a secondary reference by the substitution method. The ^{13}C 90° pulse width and the initial Hartmann–Hahn matching condition were determined by using the hexamethylbenzene standard sample.

For routine spectra of neat and supported organoactinides, the optimum cross-polarization contact time was found to be 4.0–4.5 ms (7-mm probe) and 2.5 ms (5-mm probe). The optimum recycle time was found to be 4–5 s. For neat organoactinide complexes, satisfactory spectra could be obtained by coaddition of 100–500 transients, while for supported organoactinides, the coaddition of 5000–15 000 transients was necessary. Before Fourier transformation, all FID's were weighted with a standard apodization function, $\exp(-t^2/a^2)$, where a = 0.04 s for neat organoactinides (~3 Hz line broadening) and a = 0.003 s for supported organoactinides (~120 Hz line broadening).

Because of the paramagnetism, atypical methods were necessarily employed to obtain Cp′$_2$U($^{13}CH_3$)$_2$ ^{13}C NMR spectra. The solution $^{13}C\{^1H\}$ spectrum (C_6D_6) of Cp′$_2$U($^{13}CH_3$)$_2$ was measured on the JEOL FX90 using a 50 kHz window. The U-$^{13}CH_3$ resonance was located at δ 1480, and variation of the transmitter offset confirmed that this peak was not a foldover. The Cp′–CH_3 resonance was located at δ −30, and the Cp′–C signal was not observed. In the solid-state ^{13}C CPMAS NMR spectrum of Cp′$_2$U($^{13}CH_3$)$_2$ obtained by the standard procedure (vide supra), the Cp′–CH_3 resonance was very broad (2500 Hz) and appeared at δ −32. No other resonances were observable by using CP techniques, presumably due to the short ^{13}C T_1's. However, the U–$^{13}CH_3$ resonance could be observed by application of simple 90° ^{13}C observation pulses combined with dipolar ^1H decoupling and MAS. This resonance evidenced an extensive manifold of spinning sidebands, and the largest possible spectral window was employed (100 kHz). The spectrum was referenced by setting the upfield edge of the window to δ 200 by using the carbonyl resonance of liquid acetone (δ 205.4) as a secondary reference. With this external referencing, the U-$^{13}CH_3$ isotropic chemical shift was located at δ 1430 and confirmed by varying both the transmitter offset and the spinning speed. Unfortunately, the spectral window was not large enough to encompass the entire sideband pattern.

Results and Discussion

We begin with a structurally oriented discussion of the ^{13}C CPMAS NMR spectroscopy of Cp′$_2$Th($^{13}CH_3$)$_2$ adsorbed on various dehydroxylated (i.e., having the lowest surface OH coverage readily achievable by thermal or chemical means) supports. We then probe the generality of selected aspects of the surface chemistry by using Cp′Th($^{13}CH_2C_6H_5$)$_3$, Cp$_3$Th($^{13}CH_3$), and Cp′$_2$Th($^{13}CH_2{}^{13}CH_3$)$_2$ as labeled adsorbates. Methyl group spatial relationships in surface complexes are next examined by using paramagnetic Cp′$_2$U($^{13}CH_3$)$_2$ as an adsorbate. Finally, the surface chemistry of the Cp′$_2$An($^{13}CH_3$)$_2$/support complexes is examined, in situ, with respect to ethylene polymerization and H_2, CO, and propylene reactivity.

NMR Spectroscopy of Cp′$_2$Th($^{13}CH_3$)$_2$ Adsorbed on Various Supports. Dehydration of γ-alumina at 950–1000 °C produces a mixture of γ (cubic) and δ (orthorhombic) alumina (DA) having a coverage of ~0.1 Bronsted acid OH groups, 4 Lewis base oxide groups, and 5.5 Lewis acid Al^{3+} centers nm^{-2}.[7b,8] Figure 1A shows the 75.4-MHz ^{13}C CPMAS spectrum of Cp′$_2$Th($^{13}CH_3$)$_2$ adsorbed on DA at a coverage of ca. 0.25 Th nm^{-2}. Assignments (Table I) follow straightforwardly from $^{13}C/^{12}C$ substitution, dipolar dephasing experiments,[25] and data for model compounds. The low field (δ 71.0) methyl signal is assigned to a "cation-like" Th$^+$–CH_3 functionality (cf., δ 71.8 in Cp′$_2$Th(CH_3)$^+$B(C_6H_5)$_4^-$)[13] and the upfield signal to an ^{27}Al–CH_3 functionality. This latter assignment and the quadrupole-induced broadening[26] are supported by model compounds,[12a] and the expected[26] line narrowing is observed at higher magnetic fields. Several experiments were also carried out to probe the motional characteristics of Cp′$_2$Th($^{13}CH_3$)$_2$/DA. Cessation of dipolar decoupling and Bloch decay experiments[10,27] yielded featureless spectra, while variable CP time experiments[27] (0.8–10.0 ms) produced no significant changes in relative spectral intensities. Thus, any motional processes that appreciably average C–H dipolar interactions do not differ greatly in anisotropy. Spectra of Cp′$_2$Th($^{13}CH_3$)$_2$/DA frequently exhibit a second, smaller Th–$^{13}CH_3$ signal at δ ≈ 60. This feature is the dominant Th–$^{13}CH_3$ resonance in Cp′$_2$Th($^{13}CH_3$)/PDA and is assigned to a Cp′$_2$Th(CH_3)O– μ-oxo species (B) on the basis of Cp′$_2$Th(CH_3)OR model compound data (δ 58.4 for R = CH(t-C_4H_9)$_2$).[12b] It likely arises from protonolysis[7b] by residual surface AlOH groups.

$MgCl_2$ crystallizes in the layered $CdCl_2$ structure with octahedrally coordinated Mg^{2+} cations between sheets of Cl^- anions.[28] High surface area $MgCl_2$ prepared via prolonged grinding or chemical routes has a more complex and poorly understood structural chemistry.[3,28] This material is the preferred support for "third generation" Ziegler–Natta catalysts[3] and exhibits a Lewis acid surface chemistry.[3] The spectrum of Cp′$_2$Th-

(25) (a) Alemany, L. B.; Grant, D. M.; Alger, T. D.; Pugmire, R. J. *J. Am. Chem. Soc.* **1983**, *105*, 6697–6704. (b) Opella, S. J.; Frey, M. H. *J. Am. Chem. Soc.* **1979**, *101*, 5854–5856.

(26) (a) Harris, R. K.; Nesbitt, G. J. *J. Magn. Reson.* **1988**, *78*, 245–256. (b) Jonsen, P. *J. Magn. Reson.* **1988**, *77*, 348–355. (c) Olivieri, A. C.; Frydman, L.; Grasselli, M.; Diaz, L. E. *J. Magn. Reson.* **1988**, *76*, 281–289. (d) Naito, A.; Ganapathy, S.; McDowell, C. A. *J. Magn. Reson.* **1982**, *48*, 367–381. (e) Hexanu, J. G.; Frey, M. H.; Opella, S. J. *J. Am. Chem. Soc.* **1981**, *103*, 224–226.

(27) (a) Bronnimann, C. E.; Maciel, G. E. *J. Am. Chem. Soc.* **1986**, *108*, 7154–7159. (b) Schilling, F. C.; Bovey, F. A.; Tonelli, A. E.; Tseng, S.; Woodward, A. E. *Macromolecules* **1984**, *17*, 728–733. (c) Maciel, G. E.; Haw, J. F.; Chuang, I.-S.; Hawkins, B. L.; Early, T. A.; McKay, D. R.; Petrakis, L. *J. Am. Chem. Soc.* **1983**, *105*, 5529–5535. (d) Pfeifer, H.; Meiler, W.; Deininger, D. *Annu. Rep. NMR Spectrosc.* **1983**, *15*, 291–356. (e) Duncan, T. M.; Dybowski, C. *Surf. Sci. Rep.* **1981**, *1*, 157–250.

(28) (a) Wells, A. F. *Structural Inorganic Chemistry*, 5th ed.; Oxford University Press: New York, 1984; p 350. (b) Marigo, A.; Martorana, A.; Zannetti, R. *Makromol. Chem., Rapid Commun.* **1987**, *8*, 65–68. (c) Bassi, I. W.; Polato, F.; Calcaterra, M.; Bart, J. C. J. *Z. Kristallogr.* **1982**, *159*, 297–302, and references therein.

Table I. Solid-State ^{13}C NMR Chemical Shift Data and Assignments[a]

complex	Cp′–C	An–C(α)[b]	Cp′–CH_3	others
$Cp'_2Th(^{13}CH_3)_2$	123.1	68.5	12.0	
$Cp'_2Th(^{13}CH_3)_2$/DA	124.2	71.0	10.2	−12.0 (Al–CH_3)
$Cp'_2Th(^{13}CH_3)_2/MgCl_2$	124.0	69.0	10.0	−8.0 (Mg–CH_3)
$Cp'_2Th(^{13}CH_3)_2$/DS	124.2	59.0	9.2	−5.4 (Si–CH_3)
$Cp'_2Th(^{13}CH_3)_2$/DSA		74.0	10.0	−6.0 (Al–CH_3 and/or Si–CH_3)
		60.0		
$Cp'_2Th(^{13}CH_3)_2/SiO_2$–MgO	124.1	59.1	8.7	−7.3 (Si–CH_3 + Mg–CH_3)
$Cp'_2Th(^{13}CH_3)_2$/MgO	121.3	62.1	9.8	
		55.5		
		52.3		
$Cp'_2Th(^{13}CH_3)[OSiMe_2(t\text{-}Bu)]$[c]	122.7	59.2	12.6	21.7 (*t*-Bu–CH_3), 20.3 (*t*-Bu–C), 1.1, −0.2 (Si–CH_3)
	123.4			
$Cp'_2Th(^{13}CH_3)[OCH(t\text{-}Bu)_2]$[c]	123.2	58.4	13.5	94.4 (O–CH), 38.5 (*t*-Bu–C), 30.6 (*t*-Bu–CH_3)
$Cp'_2Th(^{13}CH_3)Cl$[d]	126.3	67.6	12.5	
$Cp'_2Th(^{13}CH_3)_2$/PDA[d]	125.0	66.3	10.7	
$Cp'_2Th(^{13}CH_2{}^{13}CH_3)_2$	122.2	69.6	12.2	11.4 (Th–CH_2CH_3)
$Cp'_2Th(^{13}CH_2{}^{13}CH_3)_2/MgCl_2$	126.3	76.0	10.0	20.0 (br, Mg–CH_2CH_3, Mg–CH_2CH_3, Th–CH_2CH_3)
$Cp_3Th(^{13}CH_3)$		36.3		117.6 (Cp–C)
$Cp_3Th(^{13}CH_3)$/DA				119.2 (Cp–C)
				−15.4 (Al–CH_3)
$Cp'Th(^{13}CH_2C_6H_5)_3$	123.3	81.6	13.0	145–120 (C_6H_5)
		78.9		
		76.0		
$Cp'Th(^{13}CH_2C_6H_5)_3$/DA	126.8	95.0	10.1	20.2 (Al–$CH_2C_6H_5$)
		75.2		
		66.4		
$[Cp'_2Th(\mu\text{-}H)H]_2$	123.5		12.7	
$[Cp'_2Th(\mu\text{-}H)H]_2$/DA	125.6		10.7	
$[Cp'_2Th(\mu\text{-}H)H]_2/MgCl_2$	128.8		11.5	
$Cp'_2Th(CH_2CH_2CH_2CH_3)_2$	122.2	81.0	11.8	34.3, 32.1 (β and γ CH_2)
	122.7	93.8		15.3 (CH_3)
$Cp'Th(CH_2C_6H_5)(OC_6H_5)_2$	138.0	35.4		
		32.3		
$Cp'_2U(^{13}CH_3)_2$		1430	−25	
$Cp'_2U(^{13}CH_3)_2$/DA				−14.4 (Al–CH_3)
$Cp'_2U(^{13}CH_3)_2/MgCl_2$				−10.4 (Mg–CH_3)
$Cp'_2U(^{13}CH_3)_2$/DS				−7.4 (Si–CH_3)

[a] Versus external TMS. [b] σ-bonded carbon atom. [c] Reference 12b. [d] Reference 12a.

$(^{13}CH_3)_2/MgCl_2$ (Figure 1B; ca. 0.25Th nm^{-2}) is similar to that of $Cp'_2Th(^{13}CH_3)_2$/DA with a "cation-like" Th–CH_3 resonance and a Mg–CH_3 resonance at δ −8.0 (cf., δ −10.8 in solid CH_3MgBr).[29] Dipolar dephasing and $^{13}C/^{12}C$ substitution support this assignment (Table I). Interestingly, Bloch decay experiments yield a featureless ^{13}C spectrum except for a weak signal in the Mg–CH_3 region, suggesting limited isotropic mobility of these surface functionalities. The weak spectral feature at ca. δ 60 can be assigned on the basis of results with PDA (vide infra)[11a] and other supports (vide infra) to a $Cp'_2Th(CH_3)O$– species (B).[30a]

Figure 1C presents the CPMAS spectrum of $Cp'_2Th(^{13}CH_3)_2$ adsorbed on highly dehydroxylated (ca. 0.4 σ-OH nm^{-2})[30b] silica (DS; ca. 0.25Th nm^{-2}). Assignments are given in Table I. On the basis of model compounds, the resonance at δ −5.4 is ascribed to a surface Si–CH_3 functionality (cf., δ −1.0 for $^{13}CH_3Li$ adsorbed on DS).[12b] The Th–CH_3 resonance at δ 59.0 occurs at considerably higher field than is associated with "cation-like" species (vide supra), but in close proximity to δ Th–CH_3 for $Cp'_2Th(CH_3)OR'$ model complexes (δ 59.2, R′ = $Si(CH_3)_2(t\text{-}C_4H_9)$).[12b] These results are most compatible with a fully Th–O σ-bonded "μ-oxo-like" structure (e.g., D). Noteworthy in addition to the absence of a "cation-like" species is the complete lack of olefin hydrogenation activity by $Cp'_2Th(^{13}CH_3)_2$/DS.

Highly dehydroxylated SiO_2–Al_2O_3 (DSA) is a strong Lewis acid.[8] The CPMAS spectrum of $Cp'_2Th(^{13}CH_3)_2$/DSA (Figure 1D) bears similarities to those of both $Cp'_2Th(^{13}CH_3)_2$/DS and $Cp'_2Th(^{13}CH_3)_2$/DA. Peaks assignable (Table I) to Si–CH_3 (δ −6.0) and $Cp'_2Th(^{13}CH_3)O$– (δ 60.0) species are clearly discernable as is a Th–CH_3 resonance in the "cation-like" region (δ

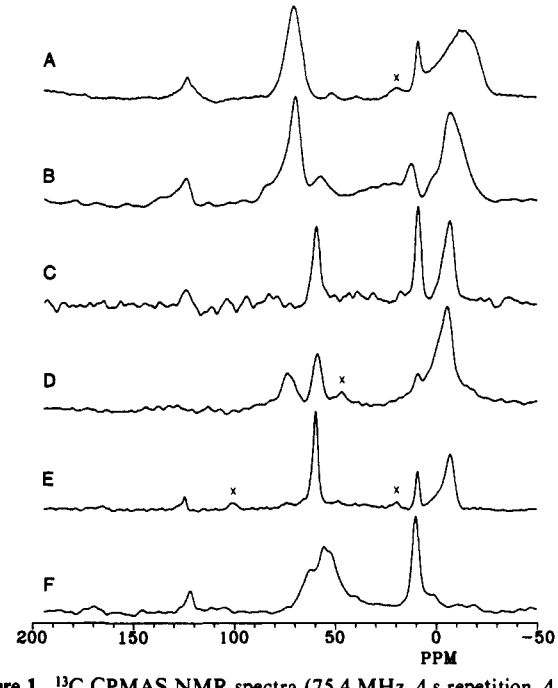

Figure 1. ^{13}C CPMAS NMR spectra (75.4 MHz, 4 s repetition, 4.5 ms contact time) of (A) $Cp'_2Th(^{13}CH_3)_2$/DA (13 200 scans), (B) $Cp'_2Th(^{13}CH_3)_2/MgCl_2$ (6050 scans), (C) $Cp'_2Th(^{13}CH_3)_2$/DS (10 125 scans), (D) $Cp'_2Th(^{13}CH_3)_2$/DSA (16 100 scans), (E) $Cp'_2Th(^{13}CH_3)_2/(SiO_2/MgO)$ (11 450 scans), and (F) $Cp'_2Th(^{13}CH_3)_2$/MgO (11 563 scans).

(29) (a) Toscano, P. J.; Marks, T. J. Unpublished results. (b) For relevant solution data, see: Leibfritz, D.; Wagner, B. O.; Roberts, J. D. *Justus Liebigs Ann. Chem.* **1972**, *763*, 173–183.

(30) (a) That initial adsorption of $Cp'_2Th(CH_3)_2$ on $MgCl_2$ releases 0.20–0.30 CH_4/Th supports the protonolytic origin of this species (Gillespie, R. D.; Marks, T. J. Unpublished results). (b) McDaniel, M. P.; Welch, M. B. *J. Catal.* **1983**, *82*, 98–109.

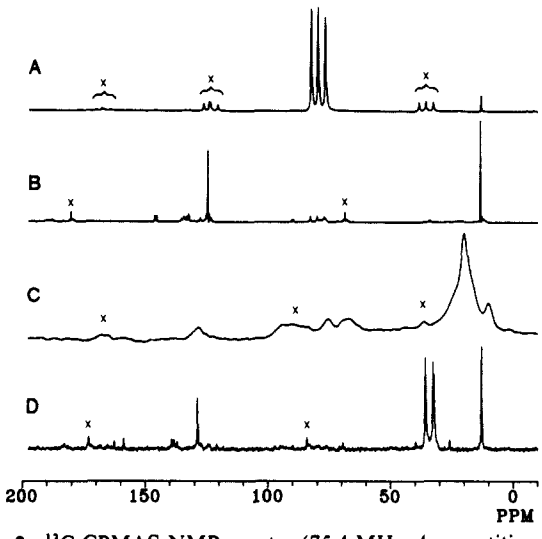

Figure 2. ^{13}C CPMAS NMR spectra (75.4 MHz, 4 s repetition time, 4.5 ms contact time) of (A) $Cp'Th(^{13}CH_2C_6H_5)_3$ as a neat solid (1220 scans), (B) $Cp'Th(CH_2C_6H_5)_3$ as a neat solid (620 scans), (C) $Cp'Th\cdot(^{13}CH_2C_6H_5)_3/DA$ (3000 scans), and (D) $Cp'Th(CH_2C_6H_5)(OC_6H_5)_2$ as a neat solid (896 scans); X denotes a spinning sideband.

70.0). Although an accompanying $Al-CH_3$ functionality cannot be rigorously identified, the spectral line shape in the δ −20–20 region is consistent with the presence of an underlying, quadrupolar-broadened $^{27}Al-CH_3$ signal superimposed upon the narrower $Si-CH_3$ resonance. The spectrum on DSA is thus compatible with both structures A and D. $Cp'_2Th(CH_3)_2/DSA$ catalyzes the hydrogenation of propylene.[7a]

The surface of dehydroxylated SiO_2–MgO (DSM) functions as a weak Lewis acid,[8d,h] while that of MgO (NaCl crystal structure[31]) functions as a weak Lewis base.[8d,h] The CPMAS spectrum of $Cp'_2Th(^{13}CH_3)_2/DSM$ (Figure 1E, Table I) exhibits a high field resonance at δ −7.3 assignable to $Si-CH_3$ and/or $Mg-CH_3$ groups (vide supra). The $Th-CH_3$ signal at δ 59.1 is consistent with a $Cp'_2Th(CH_3)O-$ σ-bonded structure. The CPMAS spectrum of $Cp'_2Th(^{13}CH_3)_2$/partially dehydroxylated MgO (PDM, Figure 1F, Table I) provides no evidence of methyl transfer to surface Mg^{2+} centers. Rather, only relatively high field $Th-CH_3$ signals at δ 62.1, 55.5, and 52.3 are observed. These can be ascribed to $Cp'_2Th(CH_3)O-$ species with the multiplicity of $Th-CH_3$ chemical shifts presumably reflecting the heterogeneity of surface microenvironments. The basic spectral pattern is reminiscent of that exhibited by $Cp'_2Th(^{13}CH_3)_2/PDA$.[12a] Attempts to further dehydroxylate MgO by heating in flowing He at 900 °C yields a low surface area material (<10 m^2/g^{-1}) which does not adsorb significant quantities of $Cp'_2Th(^{13}CH_3)_2$. In accord with the lack of detectable "cation-like" species for $Cp'_2Th(^{13}CH_3)_2/DSM$ and $Cp'_2Th(^{13}CH_3)_2/PDM$, neither substance exhibits significant olefin hydrogenation activity.[7a]

Spectroscopy of Other Actinide Hydrocarbyls Adsorbed on Alumina and Magnesium Chloride. Figure 2A presents the ^{13}C CPMAS spectrum of solid $Cp'Th(^{13}CH_2C_6H_5)_3$. The resonances at δ 123.3 and δ 13.0 are ascribed to the Cp′–C and Cp′–CH_3 groups, respectively (Table I). The crystallographically nonequivalent[21] $Th-^{13}CH_2$ moieties give rise to the three intense signals at δ 81.8, 79.0, and 76.2; assignment is confirmed by the diminution of these features in $Cp'Th(CH_2C_6H_5)_3$ (Figure 2B). The aromatic benzyl carbon atoms give rise to several resonances in the δ 145–120 region. The CPMAS spectrum of $Cp'Th\cdot(^{13}CH_2C_6H_5)_3/DA$ is shown in Figure 2C. In addition to Cp′–C and Cp′–CH_3 resonances at δ 126.8 and 10.1, respectively, an intense $^{27}Al-CH_2$ signal is observed at δ 20.2 (δ 21.0 in $Al\cdot(CH_2C_6H_5)_3$)[32] and downfield shifted $Th-CH_2$ features at ~δ 95

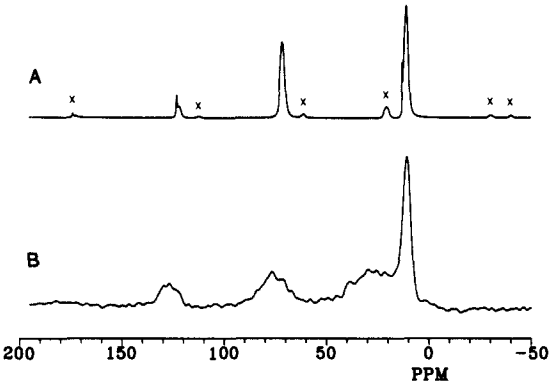

Figure 4. ^{13}C CPMAS NMR spectra (75.4 MHz, 4 s repetition time, 4.5 ms contact time) of (A) $Cp'_2Th(^{13}CH_2{}^{13}CH_3)_2$ as a neat solid (572 scans) and (B) $Cp'_2Th(^{13}CH_2{}^{13}CH_3)_2/MgCl_2$ (5620 scans).

(other $Th-CH_2-$ resonances at δ 75.2 and 66.4). The $^{27}Al-CH_2$ assignment is additionally supported by the observation of an identical feature when $Li^{13}CH_2C_6H_5$ is adsorbed on DA. These results for $Cp'Th(^{13}CH_2C_6H_5)_3/DA$ are in accord with benzyl transfer to Al^{3+} surface sites and the formation again of "cation-like" species (e.g., F). Evidence against a σ-bonded μ-oxo species (e.g., G) is provided by the spectrum of the aryloxide

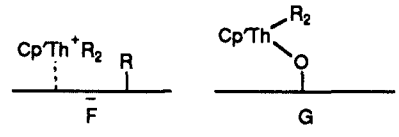

$Cp'Th(CH_2C_6H_5)(OC_6H_5)_2$[33] (Figure 2D). As in the case of $Cp'_2Th(CH_3)_2$ versus $Cp'_2Th(CH_3)OR$ (vide supra), alkoxide ligands induce an upfield displacement of hydrocarbyl α-carbon resonances. Thus, the $Th-CH_2$ signals now occur at δ 35.4 and 32.3. In accord with the "cationic" formulation for $Cp'Th\cdot(CH_2C_6H_5)_3/DA$, this material exhibits very high activity for olefin hydrogenation and polymerization (higher than $Cp'_2Th\cdot(CH_3)_2/DA$).[7b,34] However, as assayed by CO poisoning experiments, less than ~3% of the $Cp'Th(CH_2C_6H_5)_3/DA$ sites are catalytically significant.[7b]

The CPMAS spectrum of solid $Cp_3Th(^{13}CH_3)$ (Figure 3A)[35a] consists of readily assigned[35b] resonances at δ 117.6 (Cp–C) and δ 36.3 ($Th-^{13}CH_3$). When $Cp_3Th(^{13}CH_3)$ is adsorbed upon DA, the spectrum (Figure 3B, Table I)[35a] shows essentially complete transfer of the methyl groups to surface Al^{3+} sites, as evidenced by an $^{27}Al-CH_3$ resonance at δ −15.4. The Cp–C resonance is assigned at δ 119.2 with no residual $Th-CH_3$ signal detected (Table I). The formulation of surface Cp_3Th^+ cationic species (e.g., H) finds close analogy in known $(RC_5H_4)_3Th^+B(C_6H_5)_4^-$

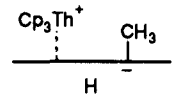

complexes.[13a] Consistent with the lack of a Th–C/H σ-bond and a high degree of coordinative saturation, Cp_3ThCH_3/DA is inactive for olefin hydrogenation except at very high temperatures.[7b]

Additional experiments were conducted on $MgCl_2$, beginning with $Cp'_2Th(^{13}CH_2{}^{13}CH_3)_2$, for reasons that will become evident in a following section. In the spectrum of neat $Cp'_2Th\cdot(^{13}CH_2{}^{13}CH_3)_2$ (Figure 4A), four resonances are observed and can be readily assigned (Table I): δ 122.2 (Cp′–C), 69.6 (Th–CH_2–), 12.2 (Cp′–CH_3), and 11.4 (Th–CH_2CH_3). $Cp'_2Th\cdot(CH_2CH_3)_2$ exhibits a similar spectrum with less intense resonances where expected. Although the Cp′ line widths are unaffected by ^{13}C enrichment, both ethyl resonances are noticeably

(31) As probed by LEED, the (100) surface of single crystal MgO differs imperceptibly from the bulk structure: Urano, T.; Kanaji, T.; Kaburagi, M. *Surf. Sci.* **1983**, *134*, 109–121.
(32) Zelta, L.; Gatti, G. *Org. Magn. Reson.* **1972**, *4*, 585–589.
(33) Sternal, R. S. Ph.D. Thesis, Northwestern University, 1988.
(34) Gillespie, R. D.; Burwell, R. L., Jr.; Marks, T. J. Unpublished results.
(35) (a) See section at end regarding Supplementary Material. (b) Fischer, R. D. In *Fundamental and Technological Aspects of Organo-f-Element Chemistry*; Marks, T. J., Fragalà, I. L., Eds.; Reidel: Dordrecht, 1985; Chapter 8, and references therein.

broader in $Cp'_2Th(^{13}CH_2{}^{13}CH_3)_2$ (~150 Hz broader with the same FID weighting). This broadening is doubtless a consequence of residual ^{13}C–^{13}C dipolar coupling[36a] that is not completely removed by the MAS employed as well as ^{13}C–^{13}C scalar coupling (anticipated to be ~35 Hz[36b]). The spectrum of $Cp'_2Th\cdot(^{13}CH_2{}^{13}CH_3)_2/MgCl_2$ (Figure 4B) is consistent with the "cation-like" model advanced for $Cp'_2Th(^{13}CH_3)_2/MgCl_2$ with Cp′–C at δ 126.3, a Th–CH_2– resonance centered at lower field (δ 76.0), a broad Mg–CH_2– resonance centered at ca. δ 20 (δ −2.9 in CH_3CH_2MgBr),[29b] and sharper coincident Th–CH_2CH_3, Mg–CH_2CH_3, and Cp′–CH_3 signals at δ 10.0 (δ 12.2 in CH_3CH_2MgBr). An alternative assignment would attribute the broad envelope at δ 40–0 to overlapping Mg–CH_2– and Mg–C·H_2CH_3 resonances, broadened by the heterogeneity of surface environments, residual ^{13}C–^{13}C dipolar coupling, and scalar coupling.

Attempts were also made to adsorb $Cp_3Th(^{13}CH_3)$ on $MgCl_2$ by using the standard procedures. However, thorough pentane washing removed all traces of the organometallic, and a CPMAS spectrum could not be detected.

A Paramagnetic Probe of Surface Alkyl–Actinide Spatial Relationships. The great bulk of Th(IV) and U(IV) organometallic chemistry is rather similar[6,19,37] as are the catalytic properties of $Cp'_2Th(CH_3)_2/DA$ and $Cp'_2U(CH_3)_2/DA$.[7b] However, U(IV) is paramagnetic ($5f^2$), and ligand resonances generally experience large paramagnetic shifts combined with relatively narrow (due to short electron spin–lattice relaxation times) line widths.[6,19,38,39] In general, the observed solution paramagnetic shifts are composed of "dipolar" (from magnetic anisotropy in the absence of cubic symmetry) and "contact" spin density delocalization (from a variety of mechanisms, including polarization of ligand orbitals by metal 6s and 6p orbitals as well as direct covalent spin density transfer from metal 5f orbitals) contributions.[38-40] Assuming a purely f orbital description for U(IV) (unquenched orbital angular momentum) and a point dipole approximation, the dipolar shift for ligand nucleus i in solution can be expressed in terms of structure-dependent geometric factors and the magnetic anisotropy of the complex (eq 1).[38,39] Here, N is Avogadro's number, the

$$\Delta H_i^{dip} = -\frac{1}{3N}[\chi_{zz} - \tfrac{1}{2}(\chi_{yy} + \chi_{xx})]\frac{3\cos^2\theta_i - 1}{r_i^3} - \frac{1}{2N}(\chi_{xx} - \chi_{yy})\frac{\sin\theta_i^2\cos 2\psi_i}{r_i^3} \quad (1)$$

χ's are magnetic susceptibility tensors, r_i is the metal-to-nuclear distance, and the angles θ and ψ fix the r_i vector within the molecular coordinate system. For axial symmetry, the expression simplifies considerably (eq 2).[38,39] In cases of axial symmetry

$$\Delta H_i^{dip} = -\frac{1}{3N}(\chi_{\parallel} - \chi_{\perp})\frac{3\cos^2\theta_i - 1}{r_i^3} \quad (2)$$

(uranocenes, Cp_3UX), it has been possible to approximately decompose the observed paramagnetic shifts into dipolar and spin

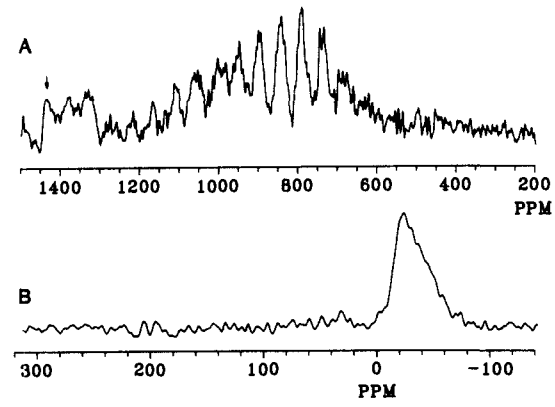

Figure 5. Solid-state ^{13}C NMR spectra (75.4 MHz) of neat $Cp'_2U\cdot(^{13}CH_3)_2$. (A) Downfield region acquired with MAS only (5 s repetition, 522 scans). The arrow indicates the centerband of the spectrum. (B) Upfield region acquired with CPMAS (5 s repetition, 4.5 ms contact time, 512 scans).

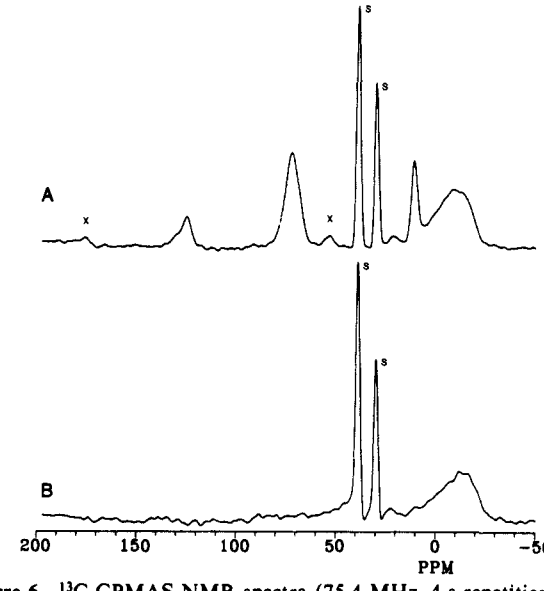

Figure 6. ^{13}C CPMAS NMR spectra (75.4 MHz, 4 s repetition time, 4.5 ms contact time) of (A) $Cp'_2Th(^{13}CH_3)_2/DA$ (1330 scans) and (B) $Cp'_2U(^{13}CH_3)/DA$ (8938 scans). Adamantane (resonances denoted by S) added as an internal intensity standard.

delocalization contributions.[39,40] No attempt has been made to perform such a decomposition for Cp'_2UR_2[15a,b,19] complexes; however, the signs and magnitudes of the observed paramagnetic shifts are roughly similar to those of the corresponding (same R) Cp_3UR complexes.[39b,c]

In randomly oriented powders or when immobilized on a surface, the ligand NMR spectra of organoactinide complexes will be modified by those anisotropic components of the dipolar[40,41] and spin delocalization[38,40] shifts which are normally averaged to zero by rapid tumbling in solution. To a first approximation, these should be similar in form to chemical shift anisotropies[42] and the anisotropic components of Knight shifts[43] and should in principal be removable (or reduced to a tractable sideband pattern)[10,43a,44] by sufficiently rapid MAS. The solution ^{13}C NMR

(36) (a) Menger, E. M.; Vega, S.; Griffin, R. G. *J. Am. Chem. Soc.* **1986**, *108*, 2215–2218, and references therein. (b) Harris, R. K. *Nuclear Magnetic Resonance Spectroscopy*; Longman Scientific: Harlow, 1986; Chapter 8–20.

(37) (a) Marks, T. J.; Ernst, R. D. In *Comprehensive Organometallic Chemistry*; Wilkinson, G. W., Stone, F. G. A., Abel, E. W., Eds.; Pergamon Press: Oxford, 1982; Chapter 21. (b) Marks, T. J.; Day, V. W. in ref 35, Chapter 4. (c) Roth, S. Ph.D. Thesis, University of Hawaii, 1988.

(38) (a) Gamp, E.; Shimomoto, R.; Edelstein, N.; McGarvey, B. R. *Inorg. Chem.* **1987**, *26*, 2177–2782, and references therein. (b) Bertini, I.; Luchinat, C. *NMR of Paramagnetic Molecules in Biological Systems*; Benjamin: Menlo Park, CA, 1986; Chapter 10. (c) McGarvey, B. R. In *Organometallics of the f-Elements*; Marks, T. J., Fischer, R. D., Eds.; Reidel Publishing Co.: Dordrecht, 1979; Chapter 10. (d) Fischer, R. D. *Ibid.* Chapter 11.

(39) (a) Luke, W. D.; Streitwieser, A., Jr. *ACS Symp. Series* **1980**, *131*, 93–140. (b) Marks, T. J.; Kolb, J. R. *J. Am. Chem. Soc.* **1975**, *97*, 27–35. (c) Marks, T. J.; Seyam, A. M.; Kolb, J. R. *J. Am. Chem. Soc.* **1973**, *95*, 5529–5539.

(40) (a) McGarvey, B. R.; Nagy, S. *Inorg. Chem.* **1987**, *26*, 4198–4203. (b) McGarvey, B. R. *Can. J. Chem.* **1984**, *62*, 1349–1355. (c) McGarvey, B. R. *J. Chem. Phys.* **1976**, *65*, 955–961. (d) McGarvey, B. R. *J. Chem. Phys.* **1976**, *65*, 962–968.

(41) Reuveni, A.; McGarvey, B. R. *J. Magn. Reson.* **1978**, *29*, 21–33.

(42) Nayeem, A.; Yesinowski, J. P. *J. Chem. Phys.* **1988**, *89*, 4600–4608, and references therein.

(43) (a) Toscano, P. J.; Marks, T. J. *J. Am. Chem. Soc.* **1986**, *108*, 437–444. (b) Reference 9b, Chapter 4. (c) Mehring, M. *Principles of High Resolution NMR in Solids*, 2nd ed.; Springer-Verlag: Berlin, 1983; Chapter 2. (d) Andrew, E. R.; Hinshaw, W. S.; Tiffen, R. S. *J. Magn. Reson.* **1974**, *15*, 191–195, and references therein.

(44) (a) Walter, T. J.; Oldfield, E. *J. Chem. Soc., Chem. Commun.* **1987**, 646–647. (b) Ganapathy, S.; Chacko, V. P.; Bryant, R. G.; Etter, M. C. *J. Am. Chem. Soc.* **1986**, *108*, 3159–3165. (c) Ganapathy, S.; Bryant, R. G. *J. Magn. Reson.* **1986**, *70*, 149–152. (d) Campbell, G. C.; Crosby, R. C.; Haw, J. T. *J. Magn. Reson.* **1986**, *69*, 191–195.

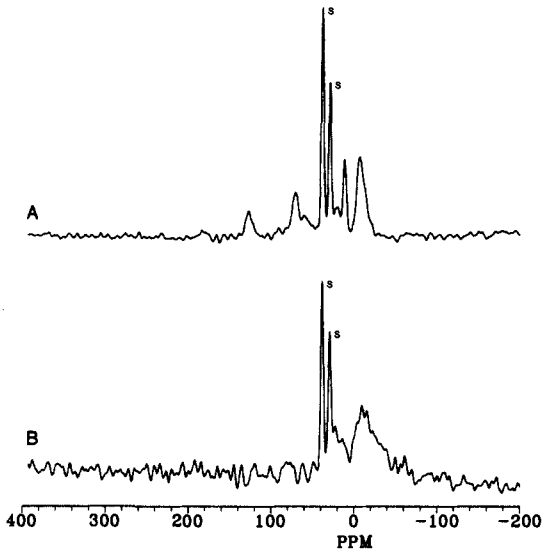

Figure 7. ^{13}C CPMAS NMR spectra (75.4 MHz, 4 s repetition time, 4.5 ms contact time) of (A) $Cp'_2Th(^{13}CH_3)_2/MgCl_2$ (2737 scans) and (B) $Cp'_2U(^{13}CH_3)_2/MgCl_2$ (5127 scans). Adamantane (resonances denoted by S) added as an internal intensity standard.

spectrum of $Cp'_2U(^{13}CH_3)_2$ exhibits a U–CH_3 resonance at δ 1480 ppm, considerably downfield from that of the diamagnetic thorium analogue (δ 68.5). Hence, the effects of the U(IV) center are extremely large for this directly σ-bonded alkyl group. The Cp′–CH_3 resonance occurs at δ −30.0, and the Cp′–C signal could not be located. For solid $Cp'_2U(^{13}CH_3)_2$, it was found that the U–CH_3 signal could be most effectively observed (presumably because of the very short T_1 and very large shift) without CP techniques. As a consequence of the large solid-state paramagnetic anisotropy, an extensive spinning sideband pattern is observed (Figure 5A). Variation of the spectral window and spinning rate allowed location of the U–CH_3 resonance at δ 1430 ± 20. Considering the slight differences in the FX90 and VXR300 probe temperatures and the experimental difficulties in acquiring the solid-state spectrum, this result is in good agreement with that in solution (δ 1480, vide supra). The Cp′–CH_3 signal could be observed by standard CPMAS as a broad peak at δ −25 (Figure 5B), only slightly displaced from the solution position (δ −30, vide supra). These results indicate that useful ^{13}C spectra of Cp'_2UR_2 complexes can be recorded in the solid state and that MAS sufficiently removes condensed phase anisotropy effects to reveal isotropic spectral features. The large shifts imparted to proximate nuclei suggest an efficacious means to probe metal–alkyl group distances on the surface.

Figure 6A and B shows CPMAS spectra of $Cp'_2Th(^{13}CH_3)_2$/DA and $Cp'_2U(^{13}CH_3)_2$/DA, respectivley, at identical loadings. Adamantane has been added as an internal standard for normalizing intensities. The spectrum of $Cp'_2U(^{13}CH_3)_2$/DA evidences no obvious Cp′U or U–CH_3 specral features either in Figure 6B or in scans over wider sweepwidths. Of course, such features are expected to be broad and rather weak under these conditions (cf., Figure 5). In contrast, the center of the Al–CH_3 signal in $Cp'_2U(^{13}CH_3)_2$/DA is only slighly displaced upfield ($\lesssim$5 ppm) from that in $Cp'_2Th(^{13}CH_3)_2$/DA, is only slightly broadened, and represents 90 ± 10% of the expected spectral intensity. If the Cp′–CH_3 resonance were present at the same field position as in neat $Cp'_2U(^{13}CH_3)_2$, it would be a broad envelope extending from ~δ −50–0, having ca. 1/10 the intensity of the Al–CH_3 signal, i.e., it would likely be obscured by the Al–CH_3 resonance. These results indicate that little if any U(IV) unpaired spin density or magnetic anisotropy is transmitted to the majority of the Al–CH_3 moieties. In similar experiments Th, U pairs were also examined for the $Cp'_2An(^{13}CH_3)_2/MgCl_2$ (Figure 7) and $Cp'_2An(^{13}CH_3)_2/SiO_2$ (Figure 8) systems. In both cases, the surface methyl group signals experience little displacement ($\lesssim$5 ppm) and only minor broadening. In both cases, 90 ± 10% of the methyl signal intensity is accounted for. Again, little interaction is observed between the majority of surface methyl groups and the U(IV) center.

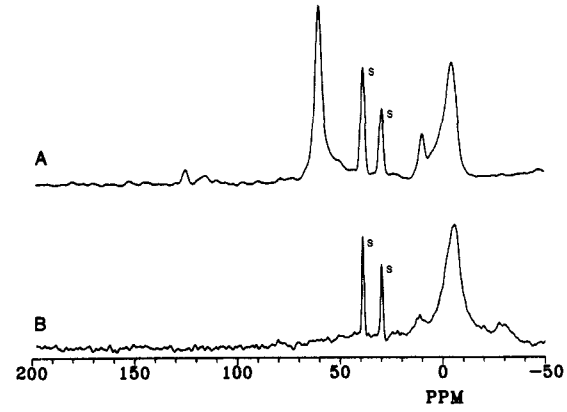

Figure 8. ^{13}C CPMAS NMR spectra (75.4 MHz, 4 s repetition time, 4.5 ms contact time) of (A) $Cp'_2Th(^{13}CH_3)_2$/DS (4668 scans) and (B) $Cp'_2U(^{13}CH_3)$/DS (10000 scans). Adamantane (resonances denoted by S) added as an internal intensity standard.

While exact quantitative analysis of U···CH_3(surface) interactions requires detailed, presently unavailable knowledge of surface $Cp'_2UCH_3^+$ magnetic anisotropy and spin delocalization, it is still possible to make physically reasonable, qualitative estimations of the range of possible U···CH_3(surface) distances. In doing so, it is pragmatically assumed that spin delocalization and dipolar shifts are roughly similar to those in the well-studied, axially symmetric Cp_3UR series.[35b,38b,39b,c,45] That observed solution shift patterns for alkyl groups are similar in Cp_3UR and $Cp'_2UR_2/Cp'_2U(Cl)R/Cp'_2U(OR')R$ complexes[15a,19,45] argues that the sums of the spin delocalization and dipolar terms are not terribly different. Where data exist for similar ligands, U(IV)-induced spin delocalization shifts do not differ greatly.[38a,39,46] In Cp_3UCH_3 at room temperature, $\Delta H^{dip} \approx +130$ ppm (upfield) and $\Delta H^{spin\ deloc} \approx +50$ ppm (upfield; in accord with a $5f^2$ polarization mechanism).[38,39] If a similar magnetic anisotropy is assumed for $Cp'_2U(CH_3)_2$, then geometric factors (eq 2) and metrical data lead to an estimate for $\Delta H^{dip}(U-^{13}CH_3)$ of ca. +300 ppm upfield. That a large, polarization-derived downfield shift dominates the observed spectral characteristics (vide infra) should not be surprising for a directly bound nucleus.[38,39] The simplest model for adsorbate structure would involve incremental displacement of the methyl group from the U(IV) center (I). Since

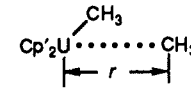

I

the spin delocalization shift is ultimately dependent on metal–ligand orbital overlap,[38,39] it is expected to attenuate far more rapidly with increasing r than the through-space dipolar term. Assuming the magnetic anisotropy and angular part of the geometric factor remain approximately constant with changing r in structure I, the question becomes how large r must become to reduce ΔH^{dip} to the magnitudes observed in the spectra of adsorbed $Cp'_2U(^{13}CH_3)_2$ (Figures 6–8). This dipolar-shift-only analysis is admittedly approximate but allows an assessment of how the surface CPMAS spectra can vary with r. Assuming that U–CH_3 = 2.43 Å in $Cp'_2U(CH_3)_2$,[37c] then the diminution ΔH^{dip} = 300 → 10 ppm corresponds to an ca. 7.6 Å increase in r. Even a more conservative 100 → 10 ppm decrease would correspond to an ca. 5.3 Å increase in r. This argument would be equally applicable to cases in which ΔH^{dip} was of opposite sign. For dynamic systems, ΔH^{dip} would be the weighted average of the spectral parameters

(45) Fagan, P. J.; Manriquez, J. M.; Marks, T. J. in ref 38c, Chapter 4.
(46) For example, in $U(H_3BC_2H_5)_4$ the spin delocalization shift of the bridging hydrogen atoms is ca. 150 ppm downfield,[38a] whereas in $Cp_3UH_3BC_2H_5$ it is ca. 60 ppm downfield.[39b]

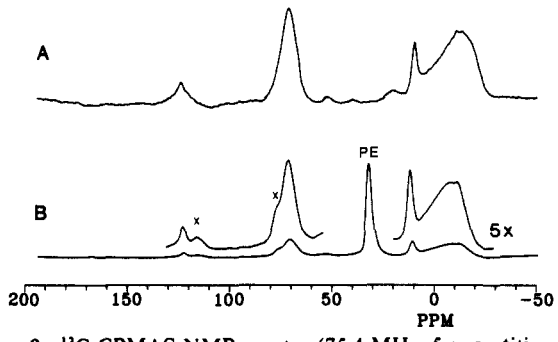

Figure 9. ^{13}C CPMAS NMR spectra (75.4 MHz, 5 s repetition time, 4.5 ms contact time) of (A) $Cp'_2Th(^{13}CH_3)_2$/DA (13 200 scans) and (B) $Cp'_2Th(^{13}CH_3)_2$/DA exposed to 30 equiv of ethylene (8835 scans). PE denotes a polyethylene $(-CH_2CH_2-)_x$ resonance, an X a spinning sideband.

in the instantaneous geometries occupied. Importantly, these results readily rule out μ-alkyl geometries such as structure E and argue that the location of the transferred methyl group on the surface must be some angstroms distant from the actinide center ($\geq$5 Å).

Adsorbate Reaction Chemistry. Ethylene. In addition to probing adsorbate structure, CPMAS NMR offers the fascinating opportunity to directly probe adsorbate reactivity. For example, the relative reactivity of An–alkyl versus surface–alkyl groups or of "cation-like" versus "μ-oxo" species can be *directly* examined via in situ competition experiments with a variety of reagents. It will be seen that the study of polymerization processes by using isotopically labeled reagents is particularly informative since the immobilized products encode "memory" effects. Experiments were first carried out in which $Cp'_2Th(^{13}CH_3)_2$/support systems were incrementally dosed with measured amounts of gaseous reagents and CPMAS spectra recorded. All possible efforts were made to rigorously exclude oxygen and water (see Experimental Section).

Ethylene polymerization was investigated by using high vacuum line experiments in which $Cp'_2Th(^{13}CH_3)_2$/support catalysts were exposed to measured quantities of ethylene. Exposures were carried out at 77 K to allow diffusion of ethylene into the pores of the catalyst prior to polymerization, thus minimizing mass transport effects. The catalyst was then slowly warmed to room temperature, during which time ethylene uptake could be detected manometrically. The $Cp'_2Th(^{13}CH_3)_2$/DA + ethylene system (Figure 9) reveals that incremental doses of olefin result in the growth of polyethylene resonances, with PE–CH_2– expected at δ 33 and PE–CH_3 expected at δ 10–15 (degenerate with the Cp′–CH_3 signal),[47] but induces no perceptible changes in the $Cp'_2Th(^{13}CH_3)_2$/DA spectrum. Since insertion of ethylene into a Th–$^{13}CH_3$ or Al–$^{13}CH_3$ bond would result in large $^{13}CH_3$ chemical shift displacements, and since no obvious diminution of relative signal intensities is evident, it is concluded that only a small percentage of the surface sites is responsible for the polymerization ($\lesssim$10%). Importantly these results agree well with the aforementioned carbonylation and protonolysis poisoning assays[7a,b] of the active site percentages, i.e., $\lesssim$4%. As a point of reference, note that at room temperature in toluene solution, neither $Cp'_2Th(CH_3)_2$ nor typical $Cp'_2Th(CH_3)X$ compounds (X = alkoxide, Cl, O_3SCF_3) undergo significant reaction with ethylene (1 atm) over the course of several hours. However, the cationic complex $Cp'_2Th(CH_3)^+B(C_6H_5)_4^-$ catalyzes ethylene polymerization with $N_t \approx 1$ min^{-1}.[12]

Ethylene dosing experiments were also conducted with $Cp'Th(^{13}CH_2C_6H_5)_3$/DA and $Cp_3Th(^{13}CH_3)$/DA. In the former case, the growth of polyethylene signals was detected, but no change in either Th–$^{13}CH_2$– or Al–$^{13}CH_2$– resonances could be observed. Again, polymerization is deduced to occur at only a small percentage of the surface sites, in agreement with catalytic poisoning assays.[7b] Exposure of $Cp_3Th(^{13}CH_3)$/DA samples to ethylene doses under identical conditions results neither in the development of polyethylene signals nor in alteration of the existing adsorbate spectrum. This result is also in accord with results of catalytic studies[7b] and with a polymerization mechanism requiring an initiating, surface Th–alkyl or Th–H functionality.

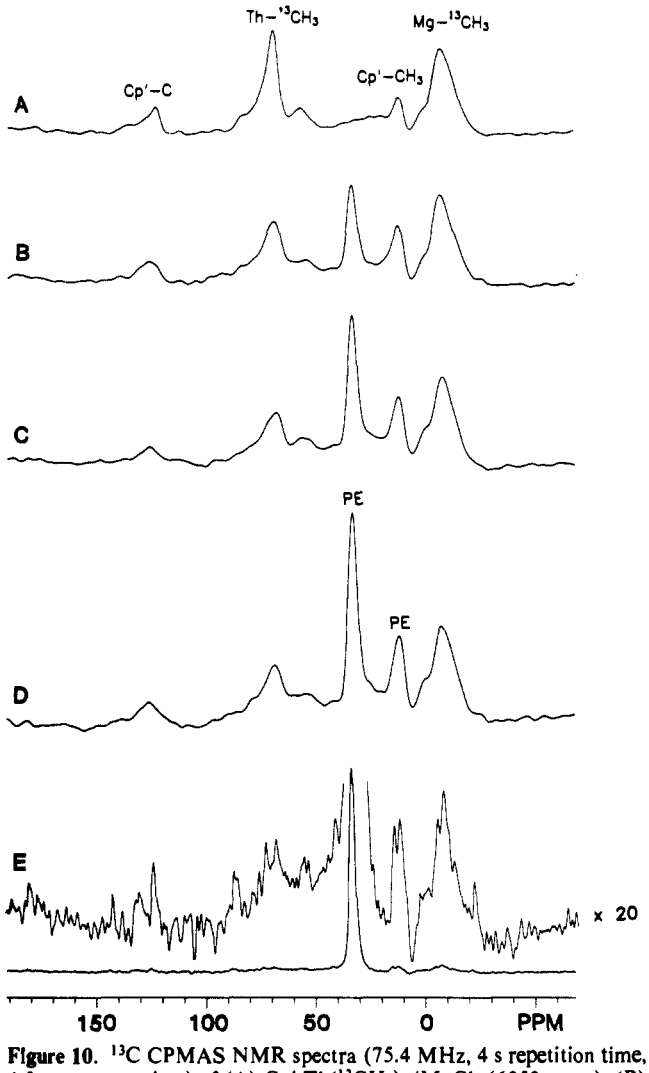

Figure 10. ^{13}C CPMAS NMR spectra (75.4 MHz, 4 s repetition time, 4.5 ms contact time) of (A) $Cp'_2Th(^{13}CH_3)_2/MgCl_2$ (6050 scans), (B) $Cp'_2Th(^{13}CH_3)_2/MgCl_2$ exposed to 5.0 equiv of ethylene (5700 scans), (C) $Cp'_2Th(^{13}CH_3)_2/MgCl_2$ exposed to 10.0 equiv of ethylene (5700 scans), (D) $Cp'_2Th(^{13}CH_3)_2/MgCl_2$ exposed to 16.0 equiv of ethylene (5900 scans), and (E) $Cp'_2Th(^{13}CH_3)_2/MgCl_2$ exposed to 350 equiv of ethylene (6000 scans). PE denotes the location of a polyethylene signal.

In principal, it should be possible to estimate the degree of ethylene polymerization from these CPMAS spectra via the relative intensities of the CH_2 and CH_3 signals. However, since longer chains will have considerable mobility, which in turn will degrade CP efficiency,[27,47] we are reluctant to quantitatively analyze such data without exhaustive calibration studies. Furthermore, as noted above, the Cp′–CH_3 and PE–CH_3 signals are nearly coincident.

One characteristic of $MgCl_2$-supported Ziegler–Natta catalysts vis-à-vis those supported on more conventional materials (e.g., Al_2O_3, SiO_2) is a far higher percentage of active sites.[3] This effect is also observed in catalytic studies of $MgCl_2$-supported organoactinides.[7a] The results of progressively dosing a $Cp'_2Th(^{13}CH_3)_2/MgCl_2$ catalyst with ethylene are shown in Figure 10. In contrast to $Cp'_2Th(^{13}CH_3)_2$/DA + ethylene, the development of polyethylene resonances is accompanied by an unambiguous initial decay of the Th–$^{13}CH_3$ signal relative to the Cp′–C resonance. The intensity of this signal continues to fall with ethylene dosing, finally levelling off at ~50% of the initial signal area relative to Cp′–C. During this same period, the polyethylene–CH_2 resonance continues to increase in relative intensity, while that

(47) Vander Hart, D. L.; Pérez, E. *Macromolecules* **1986**, *19*, 1902–1909, and references therein.

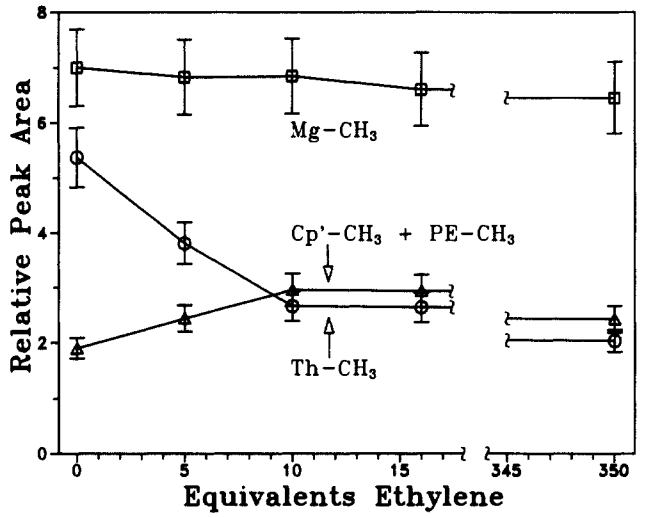

Figure 11. Relative CPMAS spectral peak areas of a $Cp'_2Th(^{13}CH_3)_2/MgCl_2$ sample exposed to the quantities of ethylene indicated.

of the Mg–$^{13}CH_3$ signal is essentially unchanged. Spectra of $Cp'_2Th(^{13}CH_3)_2/MgCl_2$ and $Cp'_2Th(^{13}CH_3)_2/MgCl_2$ + 5 equiv of ethylene recorded as a function of Cp contact time (1, 3.5, 4, and 9 ms) indicate that this quantitation is not adversely affected by changes in CP dynamics. Indeed, a strength of this assay is that it quantitates untransformed starting material of known CP and spin–lattice relaxation characteristics, rather than an emerging product of unknown characteristics.

Relative spectral peak areas for the $Cp'_2Th(^{13}CH_3)_2/MgCl_2$ + ethylene experiment are plotted in Figure 11 as a function of equivalents of added ethylene. It is concluded that 50 ± 10% of the Th–CH_3 sites undergo olefin insertion under the experimental conditions. This result is in favorable agreement with protonolytic poisoning experiments, which indicate 35 ± 10% of $Cp'_2Th(CH_3)_2/MgCl_2$ sites are active for propylene hydrogenation at −63 °C.[7a] In terms of selectivity, greater than 90 ± 10% of olefin insertion events take place at the surface Th–CH_3 functionality versus less than 10 ± 10% at the Mg–CH_3 bond. Furthermore, comparison of the Th–CH_3 peak intensity in Figure 11 versus the summed Cp′–CH_3 + PE–CH_3 peak intensities as a function of added ethylene provides an important self-consistency check. If PE–$^{13}CH_3$ formation only occurs at the expense of Th–$^{13}CH_3$ moieties, then the consumption of the latter species should be correlated with the formation of the former. The coincidence of the levelling-off portions of the PE–$^{13}CH_3$ and Th–$^{13}CH_3$ plots in Figure 11 substantiates this relationship. That the entirety of the Th–$^{13}CH_3$ intensity is not recovered in the PE–$^{13}CH_3$ resonance is evidence of (not surprisingly) rather different methyl group motional characteristic, hence CP efficiencies.[27,47] It is also possible to estimate $k_{propagation}/k_{initiation}$ for the polymerization via analysis of the diminution of the Th–$^{13}CH_3$ signals as a function of ethylene uptake. Assuming that 50% of the $Cp'_2ThCH_3^+$ surface sites undergo ethylene insertion at a uniform rate ($\theta_{ThCH_3}k_iP_{olefin}$), that subsequent ethylene insertions also occur at a uniform rate ($\theta_{Th(CH_2CH_2)_nCH_3}k_pP_{olefin}$), and that neither chain transfer (β-H elimination) nor chain termination is important, then eq 3 applies.[48] M is equivalents monomer consumed, I_0 is the initial equivalents of initiator (Th–CH_3) present, and f is the fraction of the initiator

$$\frac{M}{I_0 f} = -\frac{k_p}{k_i}\left[1 + \frac{\ln(1-f)}{f}\right] + 2 \qquad (3)$$

consumed. For the initial region of ethylene uptake in Figure 10 (0–5 equiv), this relationship yields $k_p/k_i \approx 12$ ($M \approx 5$; $f \approx 0.6$). This result can be compared to relative ethylene insertion rates in the analogous, homogeneous Cp'_2Sc–R system of k(R = $CH_2CH_2CH_3$)/k(R = CH_3) = 7.5 (4) at −80 °C.[51c]

An alternative or at least competing interpretation of the spectral changes observed in Figure 10 would be a vinylic C–H activation process,[16a,49-52] which would also result in ethylene-dependent decay of the Th–$^{13}CH_3$ signal (eq 4). To test such

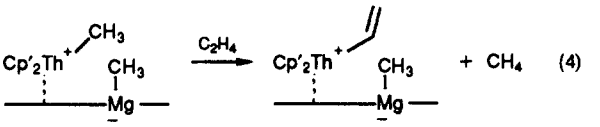

(4)

an alternative, gases evolved in the $Cp'_2Th(CH_3)_2/MgCl_2$ + ethylene reaction were collected by vacuum line techniques (77 K silica gel trap) and released as a pulse to a calibrated gas chromatography system.[7a,b] Any evolved methane was below the detection limits, hence ≲2% of the Th sites react in this manner.

The experiments of Figure 10 reveal other interesting aspects of $Cp'_2Th(^{13}CH_3)_2/MgCl_2$ surface chemistry. First, the Th–$^{13}CH_3$ feature at δ 60 assigned to a $Cp'_2Th(CH_3)O$– species (B) does not significantly change in intensity with ethylene dosing. This lower reactivity is in accord with other observations on $Cp'_2Th(OR')CH_3$ chemistry in solution.[15a,b,19] Second, these spectra and those recorded several days later evidence no perceptible variations in the residual Th–$^{13}CH_3$ and Mg–$^{13}CH_3$ spectral intensities. Thus, transalkylative exchange of Th–R and Mg–R′ groups must be slow on the time scale of days.

In principle, it should also be possible to carry out an experiment complementary to Figure 10 in which $Cp'_2Th(CH_3)_2/MgCl_2$ is incrementally dosed with $^{13}CH_2{=}^{13}CH_2$. In this case, the relative reactivity (but not the fraction of reactive sites) of the Th–CH_3 and Mg–CH_3 moieties would be monitored by the growth of the corresponding Th–$^{13}CH_2$– or Mg–$^{13}CH_2$– signals. Efforts to conduct such experiments and to observe well-resolved M–$^{13}CH_2$– signals as opposed to broad envelopes were frustrated by several factors. First, for significant degrees of ethylene polymerization, the very large $(^{13}CH_2{}^{13}CH_2)_n$ resonance creates severe dynamic range problems and spinning sidebands in the spectral region expected for the Th–$^{13}CH_2$– signal (cf., Figure 4). Secondly, the M–$^{13}CH_2{}^{13}CH_2$– resonances are expected to be broadened by ^{13}C–^{13}C scalar and unremoved dipolar coupling (vide supra).[36] Thirdly, diffraction structural, NMR spectroscopic, and theoretical results indicate that Cp'_2AnR_2 complexes occupy a very shallow potential energy surface for deformations of the Th–C(α)–C(β) valence angles.[6d,52b,53] Such distortions are frequently accompanied by C(α)H "agostic" interactions, (e.g., J). For NMR

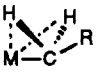

J

spectroscopy, solid-state $\delta^{13}C(\alpha)$ parameters can therefore occur over a surprisingly broad spectral range and C(α) nonequivalences are common in Cp'_2ThR_2 CPMAS spectra.[52b,54] A relevant example containing an n alkyl group is that of $Cp'_2Th(n\text{-}C_4H_9)_2$ (Figure 12,[35a] Table I). Assignment of the solution spectrum follows straightforwardly from $^{13}C\{^1H\}$ and coupled spectra: δ

(48) (a) Szwarc, M. *Adv. Polym. Sci.* **1983**, *49*, 1–177. (b) Nanda, V. S.; Jain, R. K. *J. Polym. Sci.* **1964**, *A2*, 4583–4590. (c) Litt, M. *J. Polym. Sci.* **1962**, *58*, 429–454. (d) This equation has been derived for a transferless and terminationless living polymerization in the "slow initiation" regime. Considering the substantial polydispersities observed in most heterogeneous ethylene polymerization processes,[3] the present working assumption that initiation and propagation are described by single rate constants is clearly an approximation.

(49) Rothwell, I. P. In *Activation and Functionalization of Alkanes*; Hill, C. A., Ed.; Wiley: New York, 1989; Chapter V, and references therein.

(50) Watson, P. J.; Parshall, G. W. *Acc. Chem. Res.* **1985**, *18*, 51–56.

(51) (a) Thompson, M. E.; Baster, S. M.; Bulls, A. R.; Burger, B. J.; Nolan, M. C.; Santarslero, B. D.; Schaefer, W. P.; Bercaw, J. E. *J. Am. Chem. Soc.* **1987**, *109*, 203–219. (b) Bercaw, J. E.; Davies, D. L.; Wolczanski, P. T. *Organometallics* **1986**, *5*, 443–450. (c) Parkin, G.; Bunel, E.; Burger, B. J.; Trimmer, M. S.; Van Asselt, A.; Bercaw, J. E. *J. Mol. Catal.* **1987**, *41*, 21–39. Burger, B. J.; Thompson, M. E.; Cotter, W. D.; Bercaw, J. E. *J. Am. Chem. Soc.* **1990**, *112*, 1566–1577.

(52) (a) Fendrick, C. M.; Marks, T. J. *J. Am. Chem. Soc.* **1986**, *108*, 425–437. (b) Bruno, J. W.; Smith, G. M.; Marks, T. J.; Fair, C. K.; Schultz, A. J.; Williams, J. M. *J. Am. Chem. Soc.* **1984**, *108*, 40–56. (c) Smith, G. M.; Carpenter, J. C.; Marks, T. J. *J. Am. Chem. Soc.* **1986**, *108*, 6805–6807.

(53) (a) Tatsumi, K.; Nakamura, A. *J. Am. Chem. Soc.* **1987**, *109*, 3195–3206. (b) Tatsumi, K.; Nakamura, A. *Organometallics* **1987**, *6*, 427–428.

(54) Smith, G. M. Ph.D. Thesis, Northwestern University, 1987.

122.2 (Cp′–C), 89.2 (Th–CH_3), 31.4, 31.1 (C(β) and C(α)), 14.4 (C(δ)), and 11.2 (Cp′–CH_3). The major difference in the CPMAS spectrum (Figure 12B) is the large magnetic nonequivalence observed for the C(α) resonances, viz., δ 81.0 and 93.8. Similar effects are observe in $Cp'_2Th[CH_2C(CH_3)_3]_2$ ($\Delta\delta \approx 26$) and $Cp'_2Th[CH_2Si(CH_3)_3]_2$ ($\Delta\delta = 27$) and are associated with major solid-state structural distortions (e.g., J).[6d,52b] This behavior suggests that the Th–C(α) resonances of surface-bound Th-$(^{13}CH_2{}^{13}CH_2)_nCH_3$ species are likely to occur over a broad spectral range, reflecting the modest energies required for Th–C(α)–C(β) deformation, differing n values, and the heterogeneity.

Supported organoactinide hydrides are also active olefin hydrogenation and polymerization catalysts.[7b] That the surface chemistry is similar to that of the supported hydrocarbyls is verified by CPMAS studies of $[Cp'_2Th(\mu\text{-}H)H]_2/MgCl_2$. The spectrum of the supported complex is essentially identical with that of $Cp'_2Th(^{13}CH_3)_2/MgCl_2$ except for the absence of Th–$^{13}CH_3$ and Mg–$^{13}CH_3$ signals (Table I). Dosing with ethylene gives rise to the characteristic signatures of polyethylene (Figure 13)[35a] minus, of course, the strong PE–$^{13}CH_3$ resonance previously observed at δ 12 (Figure 10). In work to be reported elsewhere,[55] we show that ^1H MAS NMR spectroscopy is an effective method to detect surface-bound organoactinide hydrides and to monitor their chemical transformations.

Additional Adsorbate Chemistry. Hydrogenolytic transformations of actinide–alkyl bonds are important in both olefin hydrogenation[4] and, for molecular weight control, in polymerization catalysis. Exposing $Cp'_2Th(^{13}CH_3)_2/DA$ samples to large molar excesses of H_2 at temperatures up to 100 °C for a period of several hours effects no perceptible changes in the CPMAS spectrum. This result agrees excellently with the low percentage of active olefin hydrogenation sites inferred from poisoning studies.[7a,b] We estimate that <10 ± 10% of the Th–CH_3 or Al–CH_3 sites undergo hydrogenolysis under these conditions. In contrast, exposure of $Cp'_2Th(^{13}CH_3)_2/MgCl_2$ to excess H_2 at room temperature for 1 h (Figure 14) results in diminution of *both* the Th–$^{13}CH_3$ and Mg–$^{13}CH_3$ signals, with the former decaying slightly more rapidly. Interestingly, samples exhibiting a significant $Cp'_2Th(^{13}CH_3)O$– resonance at $\delta \approx 60$ respond differently in that hydrogenolytic diminution of the $\delta \approx 70$ $Cp'_2ThCH_3^+$ resonance is not accompanied by a significant decay of the μ-oxo Th–$^{13}CH_3$ signal. This additional example of lower surface $Cp'_2Th(CH_3)O$– reactivity is again in accord with the solution chemistry of these less electrophilic species.[13,21] That the chemistry of Figure 14B indeed generates reactive surface hydrides is confirmed by the observation that exposure of such samples to ethylene results in the formation of polyethylene (Figure 14C).

The potency of CO as a poison of $Cp'_2Th(CH_3)_2$/support catalytic activity promoted studies with this reagent. The reaction of $Cp'_2Th(CH_3)_2/MgCl_2$ with 1 equiv of ^{13}CO (CO/Th = 1) is quantitative by manometry; however, no new ^{13}CO-derived features are evident in the δ −50–489 region of the CPMAS spectrum. In contast, exposure of $Cp'_2Th(^{13}CH_3)_2/MgCl_2$ to 1 equiv of either CO or ^{13}CO results in a nearly identical spectrum with disappearance of the Th–$^{13}CH_3$ signal, no change in the Cp′–C, Cp′–CH_3, or Mg–$^{13}CH_3$ resonances, and two new features of approximately equal intensity at δ 31 and δ 17 (Figure 15).[35a] No other resonances are observed in the δ −50–489 spectral region. Although the interpretation of these changes is not unambiguous, note that typical organothorium dihaptoacyl (K) chemical shifts are ~δ 350 (–$^{13}C(O)CH_3$) and ~δ 30 (–$C(O)^{13}CH_3$).[6b,37,45,56,57]

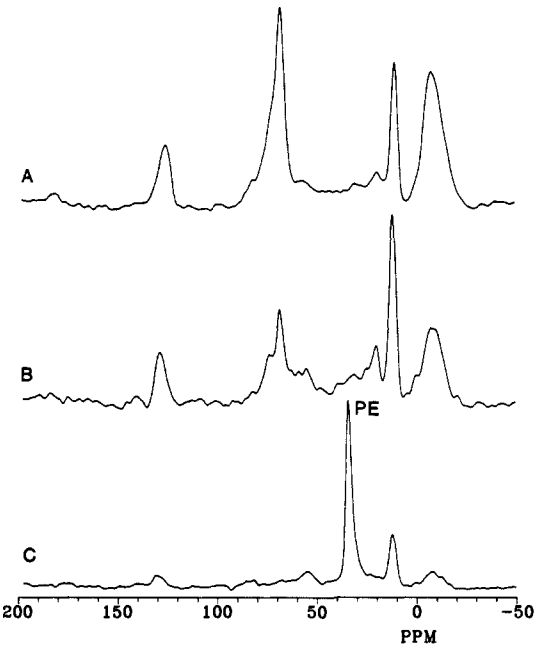

Figure 14. ^{13}C CPMAS NMR spectra (75.4 MHz, 4 s repetition time, 4.5 ms contact time) of (A) $Cp'_2Th(^{13}CH_3)_2/MgCl_2$ (8082 scans), (B) $Cp'_2Th(^{13}CH_3)_2/MgCl_2$ exposed to a large excess of H_2 (9492 scans), and (C) $Cp'_2Th(^{13}CH_3)_2/MgCl_2 + H_2$ followed by treatment with excess (20 equiv) ethylene (6220 scans).

The CSA of an acyl carbon is likely to be large, and combined with the heterogeneity of surface environments as well as possible coordination to acidic sites (e.g., L),[58] it is not surprising that this signal is not readily detected.

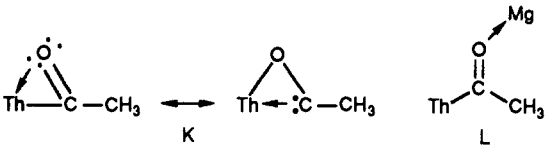

The reactivity of $Cp'_2Th(^{13}CH_3)_2/MgCl_2$ with respect to propylene was also investigated. CPMAS NMR (Figure 16A)[35a] of a sample exposed to 15 equiv of propylene (6 h at 25 °C) reveals almost complete disappearance of of Th–$^{13}CH_3$ and partial disappearance of Mg–$^{13}CH_3$. Gas-trapping/GC-based experiments reveal that under these conditions propylene exposure releases 1.1 ± 0.3 CH_4/Th. This observation suggests an allylic C–H activation process, previously observed for analogous (Cp'_2Ln-R, R = alkyl) organolanthanide complexes[59] (eq 5). Subsequent ex-

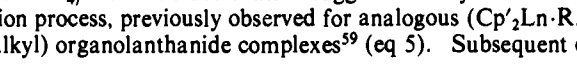

posure of this sample to H_2 (1 h at 25 °C) released 0.2 CH_4/Th, large quantities of propane and propylene, but no detectable C_4 products (isobutane, isobutylene, n-butane, etc.). Higher propylene oligomers would not be detected in this assay. Treatment with water also failed to evolve C_4 products. These results are in accord with the aforementioned NMR spectroscopic evidence (Figure 16A)[35a] for some residual surface methyl groups. Since the support was likely to have adsorbed propylene during the initial propylene dosing and since $Cp'_2Th(CH_3)_2/MgCl_2$ is a propylene hydrogenation catalyst,[7a] nothing about an η^3-allyl (eq 5) can be inferred from the C_3 products. However, the absence of isobutane argues

(55) (a) Finch, W. C.; Gillespie, R. D.; Marks, T. J. *Abstracts of Papers*, 197th National Meeting of the American Chemical Society, Dallas, TX; American Chemical Society: Washington, DC, April 9–14, 1989; INOR 33. (b) Finch, W. C.; Gillespie, R. D.; Marks, T. J. Manuscript in preparation.

(56) (a) Tatsumi, K.; Nakamura, A.; Hofmann, P.; Hoffmann, R.; Moloy, K. G.; Marks, T. J. *J. Am. Chem. Soc.* **1986**, *108*, 4467–4476, and references therein. (b) Moloy, K. G.; Fagan, P. J.; Manriquez, J. M.; Marks, T. J. *J. Am. Chem. Soc.* **1986**, *108*, 56–67, and references therein. (c) Sonnenberger, D. C.; Mintz, E. A.; Marks, T. J. *J. Am. Chem. Soc.* **1984**, *106*, 3484–3491. (d) Fagan, P. J.; Maatta, E. A.; Marks, T. J. *ACS Symp. Ser.* **1981**, *152*, 53–78. (e) Marks, T. J.; Manriquez, J. M.; Fagan, P. J.; Day, V. W.; Day, C. S.; Vollmer, S. H. *ACS Symp. Ser.* **1980**, *131*, 1–29.

(57) For example, in $Cp'_2Th[\eta^2\text{-}C(O)CH_3]^+B(C_6H_5)_4^-$, $\delta(CO) = 348.2$ and $\delta(CH_3) = 33$ (toluene-d_8 solution; Lin, Z.; Marks, T. J. Unpublished results).

(58) Waymouth, R. M.; Clauser, K. R.; Grubbs, R. H. *J. Am. Chem. Soc.* **1986**, *108*, 6385–6387.

(59) (a) Jeske, G.; Lauke, H.; Mauermann, H.; Sweptson, P. N.; Schumann, H.; Marks, T. J. *J. Am. Chem. Soc.* **1985**, *107*, 8091–8103. (b) Jeske, G.; Schock, L. E.; Swepston, P. J.; Schumann, H.; Marks, T. J. *J. Am. Chem. Soc.* **1985**, *107*, 8103–8110. (c) Jeske, G.; Lauke, H.; Mauermann, H.; Schumann, H.; Marks, T. J. *J. Am. Chem. Soc.* **1985**, *107*, 8111–8118.

against significant Th–CH_3 single step insertion chemistry (e.g., eq 6). However, the NMR feature at ~δ 25 is conceivably a

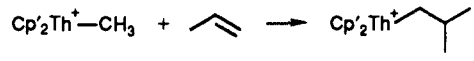

(6)

$^{13}CH_3$ end group of a propylene oligomer which would not have been detected in the trapping/GC assays (cf., δ 22.5 in solid isotactic and δ 21.0 in solid syndiotactic polypropylene[60,61]). $Cp'_2Ln(\eta^3$-allyl) and Cp'_2Ln(isobutyl) compounds are known to undergo propylene insertion (in competition with allylic C–H activation) to yield propylene oligomers.[50,59] Further support for the importance of allylic C–H functionalities here is provided by the observation that prolonged exposure of $Cp'_2Th(^{13}CH_3)_2/MgCl_2$ to 3,3'-dimethylbutene has no effect on the CPMAS spectrum (eq 7).

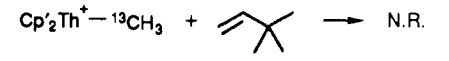

(7)

Additional information on the $Cp'_2Th(^{13}CH_3)_2/MgCl_2$ + propylene reaction is provided by studies with propylene 60% ^{13}C labeled in the C-2 position. The CPMAS spectrum (Figure 16B)[35a] reveals a multiplicity of resonances in the δ 20–70 and δ 120–150 regions. The most straightforward interpretation is in terms of repetitive propylene insertion by a surface η^3-allyl (M) to yield a mixture of oligomers (eq 8) of varying chain length (note

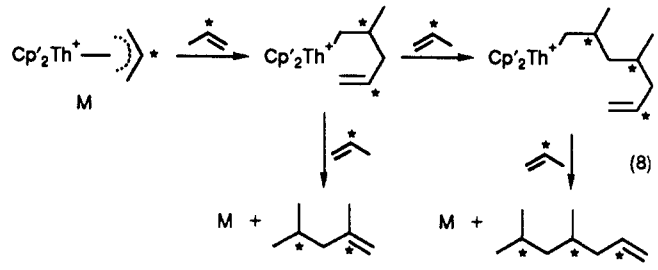

(8)

that an η^3-allyl can be regenerated via a competing process[59] analogous to eq 5), end group, and stereo- and possibly regioregularity. Thus, spectral features in the δ 140–155 region can be assigned to C2 resonances of an η^3-allyl (δ 147.3 and δ 153.3 in solid $Cp'Th(\eta^3\text{-}C_3H_5)_3$[33,62]) or to the C2 carbon of an olefinic end group (cf., eq 8; δ 140–145 in analogous olefins[63]). The resonance at ~δ 60 is assigned to an unreactive $Cp'_2Th(^{13}CH_3)O$– species, while the signals in the δ20–45 region must be due, predominantly, to labeled positons of propylene oligomers. Note that methine resonances in regioirregular polypropylenes fall in the range ~δ 28.3–38.5 in solution.[61] It is conceivable that lower molecular weights, different chain folding on the surface, olefin isomerization, and possible chemisorptive interactions with the surface[8] would increase the chemical shift dispersion further.

Conclusions

The results of this chemical/spectroscopic investigation considerably amplify what is known about organoactinide hydrocarbyl adsorbate structure and reactivity. Connections have been drawn between catalysis and spectroscopy which also convey implications for other adsorbed hydrocarbyl systems.[3]

Basically, three CPMAS spectroscopic patterns are observed for supported actinide hydrocarbyls. On strong Lewis acids (DA, $MgCl_2$, DSA), transfer of alkyl groups to acceptor sites on the surface is observed and is accompanied by residual low field Th–$^{13}C(\alpha)H_2R$ adsorbate resonances. The nature of the surface receptor site and NMR spectral similarities to species such as $Cp'_2Th(CH_3)^+BPh_4^-$ and $Cp'_2Th(CH_3)(THF)_2^+BPH_4^-$[13] suggest "cation-like" character. The present work shows this pattern is generalizable to other supports ($MgCl_2$, DSA), complexes ($Cp'ThR_3$, Cp_3ThR), and hydrocarbyl groups (ethyl, benzyl). From NMR experiments using paramagnetic U(IV) probes, it can be surmised that the great majority of $Cp'_2Th(CH_3)_2$-derived adsorbate molecules on both DA and $MgCl_2$ are not μ-alkyls (E) but rather the transferred surface alkyl moiety is $\gtrsim$5 Å displaced from the actinide center. The second type of CPMAS pattern is observed on hydroxylated supports (PDA, PDS, MgO) where it is known[7] that extensive An–R protonolysis occurs. Here, the Th–$^{13}C(\alpha)H_2R$ resonance is at considerably higher field (in the region of $Cp'_2Th(CH_3)O$-type complexes), and no transferred surface alkyl group is evident. A "μ-oxo-like" structure (B, C) is suggested for these adsorbates. Traces of these structures are occasionally observed on Lewis acid supports and provide an interesting reactivity comparison. The third type of spectroscopic pattern is observed on dehydroxylated supports without strong Lewis acid character and having relatively weak surface metal–oxygen bonds (DS, portions of the DSA surface). Here both a "μ-oxo-like" Th–$^{13}C(\alpha)H_2R$ resonance *and* a transferred surface alkyl resonance are observed, suggesting a structure such as D. Paramagnetic probes indicate that the majority of the surface alkyl groups are $\gtrsim$5 Å from the actinide center.

In regard to heterogeneous olefin hydrogenation and polymerization catalysis, the present NMR results add considerably to the structure-catalytic activity picture that is emerging. Importantly, significant catalytic activity is only observed in systems exhibiting "cation-like" spectral signatures[11e,13] (and metal alkyl or hydride bonds to effect the catalysis), while negligible activity is observed in systems exhibiting only "μ-oxo-like" ($Cp'_2Th(CH_3)O$–) spectral features.[12b,19] Moreover, "μ-oxo-like" species do not display significant reactivity in direct competition with "cation-like" species on the same surface. These reactivity trends accord well with solution chemical expectations.[6,13,14,15,19] Furthermore, the fractions of surface organoactinide complexes reactive in stoichiometric dosing experiments monitored by NMR are in good agreement with percentages of active sites assayed by catalytic CO and/or H_2O poisoning experiments.[7a,b] Thus, only ~4% of $Cp'_2Th(CH_3)_2$/DA sites are important in propylene hydrogenation and ethylene polymerization as deduced by catalytic poisoning,[7a,b] while the present NMR studies evidence ethylene polymerization by a fraction of sites below the detection limit (Figure 9; $\lesssim$10% of the total) and response to hydrogenolysis at the same level. In contrast, 35 ± 10% of $Cp'_2Th(CH_3)_2/MgCl_2$ sites are found to be significant for propylene hydrogenation by catalytic poisoning,[7a] while the present NMR studies show 50 ± 10% of the observed sites active for ethylene insertion (Figures 10 and 11) and a comparable or larger percentage reactive with respect to hydrogenolysis (Figure 14).

The gross structural formulation for alkyl-transferred surface sites as "cation-like" (A) follows from chemical, structural, and spectroscopic analogies to solution chemistry.[13,14] Not surprisingly, the chemical properties of a particular "cation-like" adsorbate are expected to be highly dependent upon the characteristics of the local counterion—in this case, the local support microstructure. This surface is not expected to be topologically uniform[8] and it is likely, depending upon the bulk support structure and local heterogeneities, that different adsorbate sites will experience different counterion/surface interactions. The present results for spectroscopically "cation-like" $Cp'_2Th(CH_3)_2$/DA and $Cp'_2Th(CH_3)_2/MgCl_2$ adsorbates underscore this point, and solution[12,13,64,65] results tell us that a completely noncoordinating anion

(60) (a) Bunn, A.; Cudby, M. E. A.; Harris, R. K.; Packer, K. J.; Say, B. J. *J. Chem. Soc., Chem. Commun.* **1981**, 15–16. (b) Bunn, A.; Cudby, M. E. A.; Harris, R. K.; Packer, K. J.; Say, B. J. *Polymer* **1982**, *23*, 694–698.

(61) Asakura, T.; Nishiyama, Y.; Doi, Y. *Macromolecules* **1987**, *20*, 616–620, and references therein.

(62) For additional η^3-allyl ^{13}C NMR data, see: Mann, B. E.; Taylor, B. F. *^{13}C NMR Data for Organometallic Compounds*; Academic Press: New York, 1981; pp 200–209.

(63) Silverstein, R. M.; Bassler, G. C.; Morrill, T. C. *Spectrometric Identification of Organic Compounds*, 4th ed.; Wiley: New York, 1981; Chapter 5.

(64) (a) Miller, P. K.; Abney, K. D.; Rappé, A. K.; Anderson, O. P.; Strauss, S. H. *Inorg. Chem.* **1988**, *27*, 2255–2261. (b) Colsman, M. R.; Noirot, M. D.; Miller, M. M.; Anderson, O. P.; Strauss, S. H. *J. Am. Chem. Soc.* **1988**, *110*, 6886–6888. (c) Moirot, M. D.; Anderson, O. P.; Strauss, S. H. *Inorg. Chem.* **1987**, *26*, 2216–2223, and references therein.

(65) (a) Liston, D. J.; Reed, C. A.; Eigenbrot, C. W.; Scheidt, W. R. *Inorg. Chem.* **1987**, *26*, 2739–2740. (b) Shelley, K.; Reed, C. A.; Lee, Y. J.; Scheidt, W. R. *J. Am. Chem. Soc.* **1986**, *108*, 3117–3118. (c) Shelley, K.; Finster, D. C.; Lee, Y. J.; Scheidt, W. R.; Reed, C. A. *J. Am. Chem. Soc.* **1985**, *107*, 5955–5959.

is difficult to achieve.

Further surface-solution chemistry connections are seen in $Cp'_2Th(CH_3)_2/MgCl_2$ CO dosing experiments, which evidence irreversible migratory insertion processes, most likely of the type previously observed in solution. $Cp'_2Th(CH_3)_2/MgCl_2$ propylene chemistry is dominated by initial allylic C-H activation/methane elimination. Subsequent chemistry involves olefin insertion and oligomerization as well as η^3-allyl formation. All of these have been previously noted in f-element solution chemistry.

Acknowledgment. We are grateful to the Division of Chemical Sciences, Office of Basic Energy Sciences, Office of Energy Research, U.S. Department of Energy, for support of this research under Grant DE-FG02-86ER13511. We thank Dr. Jean-Francois LeMarechal for generous gifts of several samples.

Supplementary Material Available: Figures 3, 12, 13, 15, and 16 showing NMR spectra (6 pages). Ordering information is given on any current masthead page.

Synthesis, Structure, and Reactivity of Metallacycle–Carbene and -Bis(carbene) Complexes. A New Intramolecular Carbene–Carbene Coupling Process

Joseph M. O'Connor,*[1a] Lin Pu,[1a,c] and Arnold L. Rheingold*[1b]

Contribution from the Departments of Chemistry, University of California at San Diego, La Jolla, California 92093, and University of Delaware, Newark, Delaware 19716.
Received November 27, 1989

Abstract: Halide ion abstraction from the neutral iridiacyclopentadiene complexes, Ir(CR=CRCR=CR)$(PPh_3)_2$Cl (**1**, R = CO_2CH_3), and Ir(CR=CRCR=CR)$(PPh_3)_2$(CO)(Cl) (**2**, R = CO_2CH_3), leads to high yields of the cationic complexes, Ir(CR=CRCR=CR)$(PPh_3)_2$(L)(L')$^+BF_4^-$ (**3**, L = CO, L' = H_2O; **4**, L = CO, L' = $NCCH_3$; **5**, L = L' = $NCCH_3$; and **6**, L = CO, L' = PMe_3). Reaction of complex **1** and 3-butyn-1-ol generates the first example of a metallacycle–carbene complex Ir(CR=CRCR=CR)$(PPh_3)_2$(Cl)[=C$(CH_2)_3$O] (**7**; 81%). Similarly, reaction of **3** or **4** and 3-butyn-1-ol leads to formation of the carbene complex Ir(CR=CRCR=CR)$(PPh_3)_2$(CO)[=C$(CH_2)_3$O]$^+BF_4^-$ (**8**; 96%). Reaction of **4** and 4-pentyn-2-ol gives a 95% yield of the substituted carbene complex Ir(CR=CRCR=CR)$(PPh_3)_2$(CO)[=C$(CH_2)_2$CHCH$_3$O]$^+BF_4^-$ (**9**). The acetonitrile analogues, Ir(CR=CRCR=CR)$(PPh_3)_2(NCCH_3)$[=C$(CH_2)_3$O]$^+BF_4^-$ (**10**) and Ir(CR=CRCR=CR)$(PPh_3)_2(NCCH_3)$[=C$(CH_2)_2$CHCH$_3$O]$^+BF_4^-$ (**11**), are also prepared in excellent yield. The bis(carbene) complex Ir(CR=CRCR=CR)$(PPh_3)_2$[=C$(CH_2)_3$O]$_2^+BF_4^-$ (**12**) is available in one step from **5** (87%). The mixed bis(carbene) complex Ir(CR=CRCR=CR)$(PPh_3)_2$[=C$(CH_2)_2$CHCH$_3$O][=C$(CH_2)_3$O]$^+BF_4^-$ (**13**) is prepared from **7** by sequential reaction with $AgBF_4$ and 4-pentyn-2-ol. Complex **8** crystallizes in space group *Cc*, with a = 12.723 (2) Å, b = 21.195 (4) Å, c = 18.432 (3) Å, β = 90.37 (1)°, V = 4970 (1) Å^3, Z = 4, $R(F)$ = 3.11%, and $R_w(F)$ = 3.76%. Complex **12** crystallizes in space group $P\bar{1}$, with a = 12.951 (2) Å, b = 13.371 (2) Å, c = 18.071 (4) Å, α = 78.42 (2)°, β = 79.27 (2)°, γ = 78.14 (1)°, V = 2966 (1) Å^3, Z = 2, $R(F)$ = 4.35%, $R_w(F)$ = 4.87%. Reaction of compounds **8** and **9** with pyridine gives the pyridinium-substituted acyl complexes Ir(CR=CRCR=CR)$(PPh_3)_2$(CO)[C(=O)$CH_2CH_2CH_2NC_5H_5$]$^+BF_4^-$ (**14**) and Ir(CR=CRCR=CR)$(PPh_3)_2$(CO)[C(=O)$CH_2CH_2CH(CH_3)NC_5H_5$]$^+BF_4^-$ (**17**). Methylamine and bis(oxacyclopentylidene) complex **12** give a nearly quantitative yield of the iridium hydride complex Ir(CR=CRCR=CR)$(PPh_3)_2(NH_2CH_3)$(H) (**19**), $CH_3NH_3^+BF_4^-$, and 2-(2(5*H*)-furanylidene)tetarhydrofuran (**20**; 92%). The mixed bis(carbene) complex **13** undergoes reaction with methylamine to give iridium hydride **19** and the carbene coupling products 2-(2(5*H*)-furanylidene)-5-methyltetrahydrofuran (**24**; 45%) and 2-(2(5-methyl)furanylidene)tetrahydrofuran (**25**; 55%). Iridium hydride **19** reacts with HCl to regenerate **1** and with HBF_4 in acetonitrile to regenerate the bis(carbene) precursor **5**. The mechanism of this novel carbene ligand coupling chemistry is discussed.

Introduction

Interest in the properties and reactivity of metal–carbene complexes has continued unabated since E. O. Fischer reported the first examples of this compound class over 20 years ago.[2] Current interest in this area stems from the role of metal carbenes in alkene metathesis,[3] alkene and alkyne polymerization,[4] and cyclopropanation chemistry,[5] and as intermediates in an impressive array of synthetic methodology.[6,7] In an effort to develop new

(1) (a) University of California, San Diego. (b) University of Delaware. (c) PRC Doering Fellow.

(2) Fischer, E. O.; Maasböl, A. *Angew. Chem.* **1964**, *76*, 645; *Angew. Chem., Int. Ed. Engl.* **1964**, *3*, 580.

(3) (a) Ivin, K. J. *Olefin Metathesis*; Academic: London, 1983. (b) Grubbs, R. H. In *Comprehensive Organometallic Chemistry*; Wilkinson, G., Stone, F. G. A., Abel, E. W., Eds.; Pergamon: New York, 1982; Vol. 8, p 499. (c) Dragutan, V.; Balaban, A. T.; Dimonie, M. *Olefin Metathesis and Ring-Opening Polymerization of Cyclo-Olefins*, 2nd ed.; Wiley-Interscience: New York, 1985.

(4) (a) Grubbs, R. H.; Tumas, W. *Science* **1989**, *243*, 907, and references therein. (b) Katz, T. J.; Lee, S. J.; Shippel, M. A. *J. Mol. Cata.* **1980**, *8*, 219. (c) Schrock, R. R.; Freudenberger, J. H.; Listemann, M. L.; McCullough, L. G. *J. Mol. Catal.* **1985**, *28*, 1. (d) Schrock, R. R. *Acc. Chem. Res.* **1986**, *19*, 342.

0002-7863/90/1512-6232$02.50/0